Atmos. Chem. Phys. Discuss., 15, 20181–20243, 2015
www.atmos-chem-phys-discuss.net/15/20181/2015/
doi:10.5194/acpd-15-20181-2015

Atmospheric Chemistry and Physics Discussions

Estimation of continuous anthropogenic CO_2 using CO_2, CO, $\delta^{13}C(CO_2)$ and $\Delta^{14}C(CO_2)$

S. N. Vardag[1], C. Gerbig[2], G. Janssens-Maenhout[3], and I. Levin[1]

[1]Institut für Umweltphysik, Heidelberg University, Heidelberg, Germany
[2]Max Planck Institute for Biogeochemistry, Hans-Knöll-Str.10, 07745 Jena, Germany
[3]European Commission, Joint Research Centre, Ispra, Via Fermi, 2749, 21027 Ispra, Italy

Received: 3 July 2015 – Accepted: 21 July 2015 – Published: 24 July 2015

Correspondence to: S. N. Vardag (svardag@iup.uni-heidelberg.de)

Published by Copernicus Publications on behalf of the European Geosciences Union.

Abstract

We investigate different methods for estimating anthropogenic CO_2 using modelled continuous atmospheric concentrations of CO_2 alone, as well as CO_2 in combination with the surrogate tracers CO, $\delta^{13}C(CO_2)$ and $\Delta^{14}C(CO_2)$. These methods are applied at three hypothetical stations representing rural, urban and polluted conditions. We find that independent of the tracer used, an observation-based estimate of continuous anthropogenic CO_2 is not feasible at rural measurement sites due to the low signal to noise ratio of anthropogenic CO_2 estimates at such settings. At urban and polluted sites, potential future continuous $\Delta^{14}C(CO_2)$ measurements with a precision of 5 ‰ or better are most promising for anthropogenic CO_2 determination (precision ca. 10–20 %), but the insensitivity against CO_2 contributions from biofuel emissions may reduce its accuracy in the future. Other tracers, such as $\delta^{13}C(CO_2)$ and CO could provide an accurate and already available alternative if all CO_2 sources in the catchment area are well characterized with respect to their isotopic signature and CO to anthropogenic CO_2 ratio. We suggest a strategy for calibrating these source characteristics on an annual basis using precise $\Delta^{14}C(CO_2)$ measurements on grab samples. The precision of anthropogenic CO_2 determination using $\delta^{13}C(CO_2)$ is largely determined by the measurement precision of $\delta^{13}C(CO_2)$ and CO_2. The precision when using the CO-method is mainly limited by the variation of natural CO sources and CO sinks. At present, continuous anthropogenic CO_2 could be determined using the tracers $\delta^{13}C(CO_2)$ and/or CO with a precision of about 30 %, a mean bias of about 10 % and without significant diurnal discrepancies. This allows significant improvement, validation and bias reduction of highly resolved emission inventories using atmospheric observation and regional modelling.

ACPD
15, 20181–20243, 2015

1 Introduction

Earth's carbon budget is strongly influenced by anthropogenic CO_2 emissions into the atmosphere (Keeling et al., 1996; Le Quéré et al., 2015). In order to support studies of the carbon cycle and to quantitatively determine net and gross carbon fluxes, various measurement sites monitor the atmospheric CO_2 mole fraction worldwide. In top-down approaches and in conjunction with atmospheric transport models, these CO_2 measurements are used to infer total CO_2 emissions (Bousquet et al., 2000; Gurney et al., 2002; Peylin et al., 2013), but a differentiation into biogenic, oceanic and anthropogenic CO_2 sources and sinks is not feasible with CO_2 concentration measurements alone. Inverse model studies commonly utilize anthropogenic CO_2 emission inventories to estimate anthropogenic CO_2 sources and are then able to separate anthropogenic from biogenic or oceanic carbon sink and source influences. However, currently available emission inventories exhibit large discrepancies between each other of about 10–40 % at the country level (Peylin et al., 2011), and increase further with decreasing spatial scale (Gurney et al., 2005). These discrepancies suggest that biases may be in the order of about 70–100 % for highly resolved ($0.1^\circ \times 0.1^\circ$) data sets and uncertainties (1σ) of emission inventories may be between 30–150 % (Wang et al., 2013). It is desirable to at least halve the current uncertainties as well as biases of emission inventories in order to better quantify anthropogenic and biogenic CO_2 sinks and sources separately. In this study, we seek to monitor anthropogenic CO_2 contributions continuously with a precision of about 30 % and with biases smaller than 10 %. Note, that we hereafter refer to anthropogenic CO_2 as fuel CO_2 and include non-combustion emissions such as emissions from cement industry or non-energy use of fuels as well as agricultural waste burning. Fossil fuel CO_2 excludes all contributions from biofuel emissions or from agricultural waste burning and thus, excludes short-cycle carbon.

^{14}C measurements are commonly used as surrogate to differentiate between biogenic and fossil fuel CO_2 contributions in the atmosphere, since fossil fuels do not contain any ^{14}C, in contrary to biogenic sources (Levin et al., 2003). The ^{14}C / C isotope

ACPD
15, 20181–20243, 2015

ratio in CO_2 is expressed on the $\Delta^{14}C(CO_2)$ scale, which denotes the deviation of the ^{14}C / C ratio in CO_2 from a standard material in permil (Stuiver and Polach, 1977). We use the depletion of $\Delta^{14}C(CO_2)$ at a polluted measurement site relative to $\Delta^{14}C(CO_2)$ in clean background air to derive quantitative information on the contribution of fossil fuel CO_2 to total measured CO_2 mole fraction at the polluted site. Radiocarbon (^{14}C) is thus used as quantitative tracer for fossil fuel contributions (Levin et al., 2003; Miller et al., 2012; Turnbull et al., 2015) and is often considered as vital for monitoring fossil fuel emissions (Miller et al., 2012). However, there are a number of problems, when using $^{14}C(CO_2)$ as tracer for anthropogenic emissions: First, precise $\Delta^{14}C(CO_2)$ measurements from conventional counting or accelerated mass spectrometry (AMS) (better than 2 ‰) are elaborate and time and cost intensive, thus currently prohibiting the coverage of large periods and large area of such measurements. Attempts have been made to sample $^{14}C(CO_2)$ in the atmosphere with a higher measurement frequency using gas chromatography (GC) coupled to continuous-flow AMS, but the precision in $\Delta^{14}C(CO_2)$ is lower than for AMS or conventional counting, which also results in less precise fossil fuel CO_2 estimates (McIntyre et al., 2013). These studies show, however, that the measurement precision using GC and continuous-flow AMS may reach 5 ‰ in near future. The benefit of such quasi-continuous but reduced precision fossil fuel CO_2 estimates is assessed for the first time in this work.

Second, a complication of applying $\Delta^{14}C(CO_2)$ measurements for fossil fuel CO_2 estimation is that nuclear power plants as well as nuclear fuel reprocessing plants emit $^{14}C(CO_2)$ and can bias regional $\Delta^{14}C(CO_2)$-based estimates of fossil fuel contributions if not taken into account (Levin et al., 2003; Graven and Gruber, 2011; Vogel et al., 2013b). Moreover, biofuel CO_2 contributions cannot be monitored with $\Delta^{14}C(CO_2)$ measurements, since they have a similar $\Delta^{14}C(CO_2)$ signature as the biosphere or may even be elevated in ^{14}C due to the bomb radiocarbon $^{14}C(CO_2)$ stored in wood material. This could become especially problematic, since the use of biofuels is expected to play an increasingly important role for the energy supply in the near future (Coyle, 2007).

ACPD
15, 20181–20243, 2015

Recognizing these shortcomings of $\Delta^{14}C(CO_2)$ as tracer for anthropogenic CO_2, it is worth considering other tracers for the estimation of fuel CO_2 contributions.

Turnbull et al. (2015) have shown that for an urban study area in the middle of the North American continent, the local CO_2 offset relative to clean air, ΔCO_2, can be used as tracer for fuel CO_2 contributions, if all other CO_2 sources and sinks, such as from the living biosphere, are negligible. This may be the case for wintertime periods in urban areas when using a background station upwind and close to the urban area. However, we do not expect ΔCO_2 to be a quantitative tracer when biospheric fluxes occur within the study area. This is normally the case in spring, summer and autumn.

Since CO is often co-emitted during (incomplete) combustion and since CO can be measured continuously, the CO offset relative to clean air, ΔCO, is frequently used as tracer for fuel CO_2 (Meijer et al., 1996; Gamnitzer et al., 2006; Rivier et al., 2006; Turnbull et al., 2006; Levin and Karstens, 2007; Vogel et al., 2010; Newman et al., 2013). If the mean ratio of the CO offset (Δx) relative to the fuel CO_2 offset (Δy_F), i.e. $\Delta x / \Delta y_F$: $= \overline{R_F}$, is known and relatively constant, it is principally possible to derive a continuous fuel CO_2 estimate from Δx measurements by dividing ΔCO by $\overline{R_F}$. The overbar shall emphasize that we use one averaged value for R_F, even though it actually varies with the relative fraction of the different emission groups in a varying catchment area of the measurement site. CO is also produced during oxidation of methane and hydrocarbons, particularly during summer. The main sinks of CO are photo-oxidation and reaction with OH (Parrish et al., 1993) as well as soil uptake (Inman et al., 1971), leading to a rather short atmospheric lifetime of CO of several weeks in summer (Prather et al., 2011). Natural CO sinks and sources vary with time and contributions of different fuel CO_2 sources, such as emissions from energy production, road traffic, residential heating and industrial emissions, with different emission ratios ($\Delta CO / \Delta CO_2$), vary during day, season as well as over longer time periods, in which combustion technologies, processes and procedures change. Therefore, the mean $\overline{R_F}$ ($= \Delta x / \Delta y_F$) is a function of space and time and might needs to be calibrated using e.g. $\Delta^{14}C(CO_2)$ measurements

ACPD
15, 20181–20243, 2015

(Levin and Karstens, 2007). If $\overline{R_F}$ does not vary significantly within the time scale of the calibration, it may then allow to estimate continuous fuel CO_2. However, if $\overline{R_F}$ varies strongly on time scales of less than the calibration interval, further corrections (e.g. diurnal or seasonal) may be necessary (Vogel et al., 2010). These corrections are only reliable if $\overline{R_F}$ variations are systematic. Since this is not always the case, additional or other continuous tracers may need to be considered to improve fuel CO_2 estimates.

One of these tracers may be $\delta^{13}C(CO_2)$, since fuel emissions tend to be more depleted in $^{13}CO_2$ than fluxes from the biosphere. Zondervan and Meijer (1996), Pataki et al. (2006) and Djuricin et al. (2010) have attempted to estimate fuel CO_2 emissions in specific case studies using mass spectrometric measurements of $\delta^{13}C(CO_2)$, in addition to $\Delta^{14}C(CO_2)$ measurements. Recently, new optical instrumentation allows measuring $\delta^{13}C(CO_2)$ continuously (e.g. Esler et al., 2000; Tuzson et al., 2011; Hammer et al., 2013; Vogel et al., 2013a) and thus open the door for $\delta^{13}C(CO_2)$ as a continuous tracer for fuel CO_2 contributions. In order to use $\delta^{13}C(CO_2)$ measurements at an urban site, the mean isotopic signature of the sources (and sinks) in the catchment area of the site, $\overline{\delta_F}$, must be known, relatively constant and potentially requires calibration (as discussed for CO). Further, the signature of fuel CO_2 emissions must be significantly different from biospheric CO_2 emissions in order to differentiate properly between them.

In many settings, we will exhibit neither a constant ratio $\overline{R_F}$ nor a constant fuel source signature $\overline{\delta_F}$. This will especially be the case if multiple sources (i) with different emission ratios $\overline{R_{F,i}}$ and different fuel $\delta^{13}C(CO_2)$ source signatures $\delta_{F,i}$ are located in the catchment area of the measurement site. In these cases, it may be advantageous to divide the fuel emissions into (two) different groups. CO will only be an adequate tracer for a certain emission group, if this group has a significantly different ratio $\overline{R_F}$ ($= \Delta x / \Delta y_F$) than any other emission group. In analogy, $\delta^{13}C(CO_2)$ will only be a good tracer for a certain emission group if the group's emissions are significantly more depleted or enriched with respect to the other groups. If we divide all

ACPD
15, 20181–20243, 2015

fuel CO_2 contributions into two emission groups, of which one is well constrained by CO and the other by $\delta^{13}C(CO_2)$, we could then join both tracers to determine the total fuel CO_2 contributions. In several published studies, the CO mole fraction has been used as a tracer for traffic contributions only (e.g. Schmidt et al., 2014), since these often exhibit high $\Delta CO / \Delta CO_2$ ratios. However, in some regions, emission inventories (e.g. Landesamt für Umwelt, Messungen und Naturschutz Baden-Württemberg, available at: http://www.ekat.baden-wuerttemberg.de/) depict that the emission ratio $\overline{R_{tr}}$ ($= \Delta x / \Delta y_{tr}$) has been decreasing during the last decade, degrading CO as a tracer for traffic contributions. At the same time, diesel/petrol for vehicle is blended with an increasing amount of biodiesel / biogasoline (to the order of 5 %). More in general, emission inventories show that biofuel CO_2 emissions have increased significantly and that the emission ratio of biofuel emissions $\overline{R_{bf}}$ ($= \Delta x / \Delta y_{bf}$) is very high, qualifying CO as a tracer for biofuel contributions. Later we examine separately, if these two emission groups, traffic and biofuel emissions, could possibly be traced with CO.

In the present study, we investigate how continuous CO_2, CO, $\delta^{13}C(CO_2)$ and $\Delta^{14}C(CO_2)$ measurements as well as the combination of these tracers could be used to estimate continuous fuel CO_2. In order to validate how precisely and accurately we may be able to determine fuel CO_2 using continuous (hourly) CO_2, CO, $\delta^{13}C(CO_2)$ and $\Delta^{14}C(CO_2)$ as tracers, we use a modelled data set, in which, contrary to measured data sets, CO_2 contributions from all source categories, i.e. the biosphere, from fossil fuel and from biofuel burning are traced separately. Using the modelled mole fractions and isotope records of CO_2, CO, $\delta^{13}C(CO_2)$ and $\Delta^{14}C(CO_2)$, we estimate the total fuel CO_2 offset using these tracers. We then discuss advantages and disadvantages of the different tracers. Using a modelled data set has the additional advantage, that isotopic signatures, emission ratios of different emission sectors etc. can be varied in order to also investigate the sensitivity of these source characteristics on the fuel CO_2 estimate. This enables us to judge how accurately the sources in the catchment of the measurement site need to be characterized for a certain required accuracy of fuel CO_2, and

ACPD
15, 20181–20243, 2015

if a calibration, using e.g. precise $\Delta^{14}C(CO_2)$ measurements, is advantageous. In the course of this, we also compare different possible sampling strategies for calibration. We further assess, which measurement precision is needed to achieve continuous fuel CO_2 estimates with sufficient precision. Additionally, we investigate the diurnal cycle of the tracer-based continuous fuel CO_2 estimates and compare them to the modelled reference fuel CO_2 in order to determine if we can reproduce the diurnal cycle correctly and hence, if we would introduce significant biases when using e.g. only afternoon values of fuel CO_2 in inverse models. We discuss the model results for a typical European urban (modelled mean fuel CO_2 offset: 16 µmol mol^{-1}), rural (modelled mean fuel CO_2 offset: 3 µmol mol^{-1}) and polluted (modelled mean fuel CO_2 offset: 25 µmol mol^{-1}) site and assess, if an estimation of continuous fuel CO_2 is possible at all sites. If this is the case, we evaluate which may be the best tracer or the best monitoring station. Finally, we give an outlook on how to apply this model study to a real measured data set.

Our investigations aim at providing the basis for the decision if continuous measurements of CO_2, CO, $\delta^{13}C(CO_2)$ and $\Delta^{14}C(CO_2)$ would be worth to be performed at a particular measurement station in order to quantitatively and precisely estimate continuous fuel CO_2 within a measurement network.

2 The modelling framework

For the study's purpose of theoretically assessing precision and accuracy of different tracer configurations for fuel CO_2 estimation, it is only of secondary importance that modelled time series are correct, but it is mainly important that the model provides a reasonably realistic data set. In this study, we simulate mole fractions and isotopic records for the Heidelberg site (49°3′ N, 8°4′ E, urban, see Levin et al., 2003) and for two non-existing stations Gartow (53°0′ N, 11°3′ E, rural) and Berlin (52°5′ N, 13°6′ E, polluted) for the year 2012. All three stations may potentially be part of the German ICOS atmospheric network (see http://www.icos-infrastructure.eu/).

ACPD
15, 20181–20243, 2015

We used the Stochastic Time-Inverted Langrangian Particle Transport (STILT) model (Lin et al., 2003) as well as pre-set source and sink distributions (see below). To simulate the atmospheric transport we used meteorological fields from the European Center for Medium-Range Weather Forecast with 3-hourly temporal resolution and 25 km × 25 km spatial resolution (Trusilova et al., 2010). By emitting 100 particles at the measurement location and inverting the meteorological fields in time, it is possible to follow the particles backward in time and track the location of their original emission. The sensitivity of the measured mole fraction at the measurement site to emissions located upstream is called footprint. The particles are traced back in time until they leave the model domain, which extends from 16° W to 36° E and from 32° N to 74° N. Initial/lateral CO_2 tracer boundary conditions for CO_2 tracer far-field mole fractions are taken from analyzed CO_2 fields, generated by the global atmospheric tracer transport model, TM3 (Heimann and Körner, 2003), based on optimized fluxes (Rödenbeck, 2005) transported at a spatial resolution of 4° × 5° with 19 vertical levels, and a temporal resolution of 6 h (s96 v3.6, http://www.bgc-jena.mpg.de/~christian.roedenbeck/download-CO2-3D/). The dynamic grid resolution in STILT is 1/12° × 1/8° (about 10 km × 10 km) close to the measurement location, and increases further away (Gerbig et al., 2006). The so-called footprint is multiplied with the biospheric and anthropogenic surface emissions to estimate the mole fraction change at the measurement site.

For the biospheric CO_2 fluxes, we use the vegetation photosynthesis and respiration model (VPRM, Mahadevan et al., 2008). The Net Ecosystem Exchange is calculated for different biome types based on SYNMAP (Jung et al., 2006) using land surface water index and enhanced vegetation index from MODIS (http://modis.gsfc.nasa.gov/) satellite data, as well as air temperature and short wave radiation from ECMWF. VPRM are computed at 1/12° × 1/8° resolution with hourly temporal resolution. We neglect biospheric CO and CH_4 fluxes in the model. CO destruction by OH and CO production via CH_4 oxidation is taken into account (Gerbig et al., 2003). However, CO production via

ACPD
15, 20181–20243, 2015

non-methane hydrocarbon (NMHC) oxidation and CO uptake by soils (Conrad, 1996) are not included in the model.

Anthropogenic emissions of CO_2, CO and CH_4 are from a preliminary version of the EDGARv4.3 emission inventory (EC-JRC/PBL, 2015), also used for the UNEP Emissions Gap Report (Rogelj et al., 2014) for the base year 2010 and have a spatial resolution of $0.1^\circ \times 0.1^\circ$. The emissions are further separated following IPCC emission categories, which are again separated in fuel types (i.e. hard coal, brown coal, oil, natural gas, derived gas, biofuels etc.). To extrapolate the emissions to the year 2012 specifically we follow the approach taken in the COFFEE dataset (CO_2 release and Oxygen uptake from Fossil Fuel Emission Estimate) (Steinbach et al., 2011) and use specific temporal factors (seasonal, weekly and daily cycles) (Denier van der Gon et al., 2011) for different emission categories, and apply country and fuel type specific year-to-year changes at national level taken from the BP statistical review of World Energy 2014 (available at: http://www.bp.com/en/global/corporate/about-bp/energy-economics/statistical-review-of-world-energy.html).

The STILT model calculates the total trace gas mole fraction of CO_2 (y_{tot}) at the measurement site as the sum of a background mole fraction y_{bg}, contributions from the biosphere y_{bio}, from different fossil fuel types $y_{ff,i}$ and different biofuel types $y_{bf,j}$:

$$y_{tot} = y_{bg} + y_{bio} + \sum_i y_{ff,i} + \sum_j y_{bf,j} \quad (1)$$

The last two terms of Eq. (1) form the total fuel CO_2 (y_F). We can associate a total isotopic $\delta^{13}C(CO_2)$ (δ_{tot}) record to the total CO_2 record following Mook (2001):

$$\delta_{tot} y_{tot} \approx \delta_{bg} y_{bg} + \delta_{bio} y_{bio} + \sum_i \delta_{ff,i} y_{ff,i} + \sum_j \delta_{bf,j} y_{bf,j} \quad (2)$$

The isotopic signatures attributed to the different emission types, e.g. $\delta_{ff,i}$ and δ_{bio} are listed in Table 1 and are independent on the emission category. Note that we do not implement a diurnal cycle into the biospheric signature.

ACPD
15, 20181–20243, 2015

The total CO mole fraction (x_{tot}) can be balanced in analogy to CO_2, but we neglect biospheric CO contributions as they are expected to be small:

$$x_{tot} = x'_{bg} + \sum_i x_{ff,i} + \sum_j x_{bf,j} = x'_{bg} + \sum_i \frac{y_{ff,i}}{R_{ff,i}} + \sum_j \frac{y_{bf,j}}{R_{bf,j}} \quad (3)$$

The emission ratios $\overline{R_{ff,i}}$ ($= \Delta x / \Delta y_{ff,i}$) depend on the emission category as well as fuel type and are determined by the emission characteristics (implied emission factors) given in EDGARv4.3. The footprint-weighted mean ratios, e.g. $\overline{R_F}$, are listed in Table A1 for Heidelberg. For the background values $\Delta^{14}C_{bg}$, y_{bg}, δ_{bg} and x'_{bg}, we use those mole fractions where CH_4 mole fractions reach a minimum value within two days. This is mainly the case in the afternoon when vertical mixing is strongest (for more details on the choice of background see Appendix A2). Note, that the CO background x'_{bg} is denoted with a prime, since it has been corrected for chemical reactions with OH (sink) and for production from oxidation of CH_4 by applying a first-order chemical reaction on hourly OH and CH_4 fields. The contributions of fossil fuel and biofuel CO, are, however, not corrected for these chemical reactions in the model, since the CO, which is released in the footprint area of the measurement site typically travels only a fraction of its actual life-time until arriving at the measurement site.

The $\Delta^{14}C(CO_2)$ ($\Delta^{14}C_{tot}$) balance is also simulated and follows:

$$y_{tot}\left(\Delta^{14}C_{tot}+1\right) \approx y_{bg}\left(\Delta^{14}C_{bg}+1\right) + y_{bio}\left(\Delta^{14}C_{bio}+1\right) + \sum_i y_{ff,i}\left(\Delta^{14}C_{ff,i}+1\right) + \sum_j y_{bf,j}(\Delta^{14}C_{bf,j}+1) \quad (4)$$

With $\Delta^{14}C_{bio}$, $\Delta^{14}C_{bf,j}$ and $\Delta^{14}C_{ff,i}$ listed in Table A1 and CO_2 mole fractions from model results. As all fossil fuel CO_2 sources are void of $^{14}C(CO_2)$, fuel CO_2 contributions are separated into fossil fuel and biofuel contributions.

ACPD
15, 20181–20243, 2015

In the following, we use six different tracers or tracer combinations to derive continuous fuel CO_2 (see Table 2).

The formal derivation of the continuous fuel CO_2 estimate from these six different tracers or tracer combinations can be found in the Appendix A1, where the different targeted emission groups (fuel CO_2, fossil fuel CO_2, fuel CO_2 without traffic, traffic CO_2, biofuel CO_2 and biospheric CO_2) are also listed and characterized in Table A1.

3 Results

We now investigate how well the different tracers perform at a typical urban, rural and polluted measurement site. First, we will discuss the upper limit of precision and accuracy of fuel CO_2 estimation using these tracers when assuming all parameters (e.g. $\overline{\delta_F}$) are known at every time. We then investigate how the use of averaged accurate parameters and variables affects the fuel CO_2 estimate. Next, we also perform a sensitivity analysis to identify, which parameters and variables need to be known and at which precision and accuracy for fuel CO_2 estimation with satisfying accuracy (of e.g. smaller than 10 %). Finally, we discuss the diurnal variation of fuel CO_2 and include a realistic measurement uncertainty into our considerations.

3.1 High (hourly) resolution of parameters and variables

The integrated footprint-weighted parameters (e.g. $\overline{R_F}$, $\overline{R_{tr}}$, $\overline{R_{bf}}$, $\overline{\delta_F}$, $\overline{\delta_{ff}}$, $\overline{\delta_{bf}}$, $\overline{\delta_{tr}}$, $\overline{\delta_{F\text{-}tr}}$, $\overline{m_{bf}}$ and $\overline{m_{tr}}$) are needed for the estimation of fuel CO_2 using the different tracers. However, they are dependent on the emission characteristics of the sources in the catchment area of the measurement site. If e.g. the mean isotopic signature of fuel CO_2 sources in the catchment area varies or if the catchment area itself varies, the integrated footprint-weighted parameter $\overline{\delta_F}$ will change. Typically, the integrated footprint-weighted parameters vary on time scales of hours, weeks, months and years. If, for a given measurement site, we could determine these parameters on the time scale of

ACPD
15, 20181–20243, 2015

hours (which is the temporal resolution of our model), we would be able to estimate fuel CO_2 entirely correctly (difference of estimated and modelled fuel CO_2 would be zero) using CO and $\delta^{13}C(CO_2)$ or any combination of these tracers.

In contrast to methods using CO and/or $\delta^{13}C(CO_2)$, CO_2-based estimations would overestimate fuel CO_2, when biospheric CO_2 contributions are positive (which will often be the case during night time and in winter) and underestimate fuel CO_2 when the biospheric CO_2 is negative (which may be the case during daytime in summer). This would lead to a median overestimation of fuel CO_2 by about 5 % (Berlin) to 50 % (Gartow), depending on the proportion of biospheric CO_2 to total CO_2 at the location.

As $\Delta^{14}C(CO_2)$ is not sensitive to biofuel contributions, $\Delta^{14}C(CO_2)$ based fuel CO_2 estimates will underestimate the fuel CO_2 contributions approximately by the amount of biofuel CO_2 to the regional CO_2 concentration offset. For our model runs, this leads to a median underestimation of about 5 % (Berlin) to 10 % (Heidelberg and Gartow) dependent on the share of biofuel CO_2 at the measurement site. Note, that we did not include any $^{14}C(CO_2)$ emissions from nearby nuclear power plants or nuclear fuel reprocessing plants into the considerations, which would potentially mask the depletion of fuel CO_2 contributions. However, we will discuss possible effects in Sect. 5.

Normally it will not be possible to determine parameters such as $\overline{R_F}$, $\overline{R_{tr}}$, $\overline{R_{bf}}$, $\overline{\delta_F}$, $\overline{\delta_{ff}}$, $\overline{\delta_{bf}}$, $\overline{\delta_{tr}}$, $\overline{\delta_{F\text{-}tr}}$, $\overline{m_{bf}}$ and $\overline{m_{tr}}$ with hourly resolution. We, thus, investigate how using (monthly) median values of these parameters may influence the fuel CO_2 estimates.

3.2 Low (monthly) resolution of parameters and variables

We now only use the monthly median value of the footprint-weighted parameters $\overline{R_F}$, $\overline{R_{tr}}$, $\overline{R_{bf}}$, $\overline{\delta_F}$, $\overline{\delta_{ff}}$, $\overline{\delta_{bf}}$, $\overline{\delta_{tr}}$, $\overline{\delta_{F\text{-}tr}}$, $\overline{m_{bf}}$ and $\overline{m_{tr}}$ to estimate fuel CO_2. Note, that we use the median instead of the mean value for the footprint-weighted parameters, since the median is less sensitive to outliers. Using only monthly median values will introduce sub-monthly inaccuracies into the fuel CO_2 estimate since the footprint-weighted parameters vary on sub-monthly timescales. The variability of the discrepancy be-

ACPD
15, 20181–20243, 2015

tween estimated and reference (directly modelled) fuel CO_2 estimates will depend on the magnitude of sub-monthly variations of $\overline{R_F}$, $\overline{R_{tr}}$, $\overline{R_{bf}}$, $\overline{\delta_F}$, $\overline{\delta_{ff}}$, $\overline{\delta_{bf}}$, $\overline{\delta_{tr}}$, $\overline{\delta_{F\text{-}tr}}$, $\overline{m_{bf}}$ and $\overline{m_{tr}}$, but also on their absolute values. For example, the more depleted the fuel CO_2 emissions are, the larger the isotopic difference between emissions from the biosphere and from fuel burning and the better the tracer $\delta^{13}C(CO_2)$ will be for fuel CO_2 emissions as both emission groups can be isotopically distinguished clearly (see Appendix C). For our model setting, the sub-monthly variations (standard deviation) in our model runs are about $\pm 1\,(\text{nmol mol}^{-1})\,(\mu\text{mol mol}^{-1})^{-1}$ for $\overline{R_F}$, $\overline{R_{tr}}$ and $\overline{R_{bf}}$, $\pm 0.15\,(\text{nmol mol}^{-1})\,(\mu\text{mol mol}^{-1})^{-1}$ for $\overline{m_{bf}}$ and $\overline{m_{tr}}$ and ± 2 ‰ for $\overline{\delta_F}$, $\overline{\delta_{ff}}$, $\overline{\delta_{bf}}$, $\overline{\delta_{tr}}$ and $\overline{\delta_{F\text{-}tr}}$ (variations due to varying footprints in the STILT model and temporal emission patterns of the different emission sectors). This variation is propagated into the fuel CO_2 estimate. Until now, parameters such as $\delta^{13}C_{bio}$, $\Delta^{14}C(CO_2)_{bio}$ and $\Delta^{14}C(CO_2)_{bf}$ are assumed to be constant within one month, and natural CO emisisons as well as measurement uncertainties are assumed to be zero. The corresponding distribution of the difference between the estimated and modelled fuel CO_2 can be seen in Fig. 1 for the station Heidelberg, which is a typical urban measurement site with large fuel CO_2 emissions, but also similarly high biogenic sources and sinks in the catchment, which are also active during relatively mild winters. The mean modelled fuel CO_2 offset in Heidelberg is about $16\,\mu\text{mol mol}^{-1}$. We additionally show the results for the stations Gartow and Berlin (see Figs. 2 and 3, respectively). The typical rural measurement site at Gartow (53°0′ N, 11°3′ E) is located in Northern Germany about 160 km north-west from Berlin and exhibits a mean modelled fuel CO_2 of about $3\,\mu\text{mol mol}^{-1}$. The measurement site in the outskirts of Berlin (52°5′ N, 13°6′ E) has a mean modelled fuel CO_2 of $25\,\mu\text{mol mol}^{-1}$ and is considered a polluted site. For all sites, we looked at the same height above ground level as in Heidelberg (30 m a.g.l.).

The mean difference between the modelled and tracer-based fuel CO_2 estimate provides a measure for the accuracy of the fuel CO_2 determination with the different tracer methods. In principle, it is not correct to assume that, when using the correct median

ACPD
15, 20181–20243, 2015

values for $\overline{R_F}$, $\overline{R_{tr}}$, $\overline{R_{bf}}$, $\overline{\delta_F}$, $\overline{\delta_{ff}}$, $\overline{\delta_{bf}}$, $\overline{\delta_{tr}}$ and $\overline{\delta_{F\text{-}tr}}$, no median bias will be introduced into the CO_2 estimate. The reason is that the values for $\overline{R_F}$, $\overline{R_{tr}}$, $\overline{R_{bf}}$, $\overline{\delta_F}$, $\overline{\delta_{ff}}$, $\overline{\delta_{bf}}$, $\overline{\delta_{tr}}$ and $\overline{\delta_{F\text{-}tr}}$ are calculated on an hourly basis independent on the total fuel CO_2 value (y_F) at that time and are then averaged monthly. However, if y_F and $\overline{R_F}$, $\overline{R_{tr}}$, $\overline{R_{bf}}$, $\overline{\delta_F}$, $\overline{\delta_{ff}}$, $\overline{\delta_{bf}}$, $\overline{\delta_{tr}}$ and $\overline{\delta_{F\text{-}tr}}$ are correlated, sub-monthly over- and underestimation of y_F due to sub-monthly variation of for $\overline{R_F}$, $\overline{R_{tr}}$, $\overline{R_{bf}}$, $\overline{\delta_F}$, $\overline{\delta_{ff}}$, $\overline{\delta_{bf}}$, $\overline{\delta_{tr}}$, $\overline{\delta_{bio}}$ and $\overline{\delta_{F\text{-}tr}}$ will not average out necessarily. An analysis of the bias introduced when using monthly median footprint-weighted parameters is therefore vital. The standard deviations of the Gaussian fits to the difference distributions provide a measure for the precision of fuel CO_2 determination.

All methods using $\delta^{13}C(CO_2)$ (Figs. 1c–e, 2c–e and 3c–e) are able to estimate fuel CO_2 without significant systematic biases. Mean and median differences of modelled and estimated fuel CO_2 are within 10 % of the mean annual fuel CO_2 signal. The benefit when using CO additionally to $\delta^{13}C(CO_2)$ is very small, which is due to the fact that traffic or biofuel CO_2 contributions are not very distinct with respect to their isotopic signature or their CO/CO_2 emission ratio from the other fuel CO_2 contributions for our model settings (see Table A1). When using CO as tracer for fuel CO_2 (Figs. 1b, 2b and 3b) the standard deviation of the difference between the estimated and real fuel CO_2 value is slightly larger than when using $\delta^{13}C(CO_2)$. The reason is the large sub-monthly variation of footprint-weighted $\overline{R_F}$ in our modelled data.

Principally, the standard deviation of the different tracer distributions is about 40–70 % larger at the polluted station than at urban and rural stations. However, we found that the variation of the footprint-weighted parameters such as $\overline{R_F}$, $\overline{R_{tr}}$, $\overline{R_{bf}}$, $\overline{\delta_F}$, $\overline{\delta_{ff}}$, $\overline{\delta_{bf}}$, $\overline{\delta_{tr}}$, $\overline{\delta_{F\text{-}tr}}$, $\overline{\delta_{bio}}$, $\overline{m_{bf}}$ and $\overline{m_{tr}}$ is largest in rural areas and smallest in polluted areas, which is probably due to the fact that in polluted catchment areas the many polluters homogenizes partly, whereas at cleaner sites the emissions of the few different polluters are temporally and spatially distinct. Hence, the larger spread of the fuel CO_2 estimate at polluted stations is not the result of larger source heterogeneity, but is due to the larger absolute signals (and with that larger absolute variations) of fuel CO_2 in the catchment

ACPD
15, 20181–20243, 2015

area of more polluted sites. Only CO_2 as tracer for fuel CO_2 shows less variability at Berlin, which is due to smaller contribution from the biosphere in the catchment area of the polluted measurement site. However, the relative variability ($=1\sigma$ / mean(y_F)) is significantly higher in Gartow (e.g. δ^{13}C-method: 20 %) than it is in Heidelberg or Berlin (both 4 %).

We have found that only small median differences occur when using $\delta^{13}C(CO_2)$ or CO as tracer for fuel CO_2, but this finding is only valid under the premise, that the median values of all input and footprint-weighted parameters are known. If one or more of the parameters or variables are assigned incorrectly, this will lead to a systematic error of the fuel CO_2 estimate. The sensitivity of this misassignment for the different parameters and variables will be assessed in the next chapter.

3.3 Sensitivity of fuel CO_2 estimates on misassigned parameters and variables

We have investigated how well we are able to estimate fuel CO_2 in a setting in which e.g. the monthly averages of all parameters are perfectly well known, but temporally varying on shorter time scale. However, since, in reality, parameters such as $\overline{\delta_F}$ or $\overline{R_F}$ are only approximately known, we need to investigate how a misassignment of one of these parameters will influence fuel CO_2 estimates. This will provide information on how well certain parameters and variables need to be assigned for a fuel CO_2 estimate with targeted accuracy. For this purpose, we misassign one parameter and, at the same time, keep the other parameters at their correct value. We then determine how the fuel CO_2 estimate changes (y axis in Fig. 4) when the misassignment of the parameter (x axis) varies. The sensitivities of all methods to the most important parameters and variables are shown in Fig. 4 exemplary for the urban site Heidelberg. We have done this analysis for the parameters total CO_2 (y_{tot}) (Fig. 4a), $\delta^{13}C_{tot}$ (Fig. 4b), background CO_2 (y_{bg}) (Fig. 4c), $\delta^{13}C_{bg}$ (Fig. 4d), $\overline{\delta_F}$ (Fig. 4e), $\overline{\delta_{bio}}$ (Fig. 4f), $\overline{\delta_{bf}}$ (Fig. 4g), $\overline{\delta_{tr}}$ (Fig. 4h), CO offset (x) (Fig. 4i), $\overline{m_{bf}}$, $\overline{m_{tr}}$ (Fig. 4j), $\overline{R_{tr}}$, $\overline{R_{bf}}$ (Fig. 4k), $\overline{R_F}$ (Fig. 4l), $\Delta^{14}C_{tot}$ (Fig. 4m), $\Delta^{14}C_{bg}$ (Fig. 4n), $\Delta^{14}C_{bio}$ (Fig. 4o) and $\Delta^{14}C_{bf}$ (Fig. 4p). The variation of these values

ACPD
15, 20181–20243, 2015

was chosen so that the range includes the typical measurement precision for CO_{2meas}, CO_{2bg}, δ_{bg}, δ_{meas}, $\Delta^{14}C_{bg}$ and $\Delta^{14}C_{meas}$. The variation of the CO offset was chosen so that it displays the measurement precision of total CO and of the background CO, but also realistic contributions from natural CO sources and sinks. For the parameters $\overline{R_F}$, $\overline{R_{tr}}$, $\overline{R_{bf}}$, $\overline{\delta_F}$, $\overline{\delta_{ff}}$, $\overline{\delta_{bf}}$, $\overline{\delta_{tr}}$, $\overline{\delta_{bio}}$, $\overline{\delta_{F\text{-}tr}}$, $\overline{m_{bf}}$, $\overline{m_{tr}}$, $\Delta^{14}C_{bio}$ and $\Delta^{14}C_{bf}$, we selected realistic ranges of sub-monthly parameter variation.

The error bars given on the right hand side of Fig. 4 show the interquartile ranges (IQR) and stem from the sub-monthly variability of $\overline{\delta_F}$, $\overline{R_F}$, $\overline{m_{bf}}$ and $\overline{m_{tr}}$, which was discussed in Sect. 3.2. One can directly identify critical parameters and variables, for which the difference between the modelled and estimated fuel CO_2 (y axis) changes significantly with increasing misassignment of parameters/variables (x axis).

3.3.1 Sensitivity of CO_2-only method

We confirm that the CO_2-only method (green in Fig. 4) is insensitive to the variation of the displayed parameters/variables. However, the large IQR of the CO_2-only method, as well as the median overestimation of fuel CO_2 by about 2.4 µmol mol^{-1} disqualifies this method at an urban site with non-negligible biospheric influences.

3.3.2 Sensitivity of CO method

Critical parameters/variables of the CO method (orange in Fig. 4) are the CO offset ΔCO (Fig. 4i), as well as the ratio $\overline{R_F}$ (= Δx / y_F) (Fig. 4l). In practise, the CO offset is derived by subtracting the CO background as well as natural CO source and sink contributions from the total measured CO mole fraction. Typical fuel CO offsets are in the order of 40 nmol mol^{-1}. In our model we have not included natural CO sources and sinks, but in practise, the uncertainty of the CO mole fraction measurement and of the natural CO contributions will add to the uncertainty of the fuel CO_2 estimate. Assuming e.g. a CO background, which is 15 nmol mol^{-1} too large, or assuming an additional

ACPD
15, 20181–20243, 2015

sink resulting in a 15 nmol mol^{-1} lower CO background, which may be a realistic diurnal variation of natural CO variation (Gros et al., 2002; Vogel, 2010), would lead to a significant overestimation of fuel CO_2 of about 4 µmol mol^{-1} (median). Therefore, for a real data set, it is vital to determine the natural CO contributions and sinks (also soil sinks) using chemistry models or calibration with e.g. $\Delta^{14}C(CO_2)$ (see Sect. 4). In Heidelberg, the median ratio $\overline{R_F}$ is about 3.7 (nmol mol^{-1}) (µmol mol^{-1})$^{-1}$ and shows a rather large variation standard deviation of 2.3 (nmol mol^{-1}) (µmol mol^{-1})$^{-1}$. Figure 4l shows, that such a variation of $\overline{R_F}$ contributes significantly to the imprecision of fuel CO_2 in the CO-method. Also, the correct determination of $\overline{R_F}$ is vital for accurate fuel CO_2 estimates using CO.

3.3.3 Sensitivity of methods using $\delta^{13}C(CO_2)$

The sensitivities of fuel CO_2 estimates using $\delta^{13}C(CO_2)$ (red and black in Fig. 4) and combinations of $\delta^{13}C(CO_2)$ and CO are rather similar (blue in Fig. 4). Note that the sensitivity on δ_{bg} or δ_{tot} is plotted when keeping y_{bg} and y_{tot} constant. Changing the y_{bg} or y_{tot} values at the same time when changing δ_{bg} or δ_{tot} (following a Keeling curve (Keeling, 1958, 1960) with typical mean $\delta^{13}C$ source of −25 ‰) results in about a factor ten smaller sensitivity and is therefore not critical. However, small $\delta^{13}C(CO_2)$ variations (e.g. due to finite measurement precision or small inaccuracies), which are uncorrelated with total CO_2, lead to large biases in fuel CO_2, e.g. a measurement bias of δ_{tot} = 0.1 ‰ leads to a fuel CO_2 misassignment of 5 µmol mol^{-1} (see Fig. 4b). Therefore, a high measurement precision as well as accuracy of $\delta^{13}C(CO_2)$ is required for precise and accurate fuel CO_2 estimation. Further critical parameters of the methods using $\delta^{13}C(CO_2)$ are the isotopic signature of fuel CO_2 and the isotopic signature of biospheric CO_2 in the footprint (see Fig. 4e, f). The isotopic signatures of fuel and biospheric CO_2 must therefore be well known (or potentially calibrated, see Sect. 4), if we want to use $\delta^{13}C(CO_2)$ as tracer for fuel CO_2. Especially assuming more enriched

ACPD
15, 20181–20243, 2015

fuel isotopic signatures or too depleted biospheric signatures biases the fuel CO_2 estimates strongly, because in these cases, biospheric and fuel CO_2 sources are difficult to distinguish using $\delta^{13}C(CO_2)$.

3.3.4 Sensitivity of $\Delta^{14}C(CO_2)$ method

Figure 4m–p display the sensitivity of the $\Delta^{14}C(CO_2)$ based estimate of fuel CO_2 on the variables $\Delta^{14}C_{tot}$, $\Delta^{14}C_{bg}$ and $\Delta^{14}C_{bio}$. While fuel CO_2 is rather insensitive against misassignment of $\Delta^{14}C(CO_{2bio})$ (Fig. 4o) and $\Delta^{14}C(CO_2)_{bf}$ (Fig. 4p), it is very sensitive on $\Delta^{14}C(CO_2)_{tot}$ (Fig. 4m) and $\Delta^{14}C(CO_{2bg})$ (Fig. 4n). Thus, precise and accurate $\Delta^{14}C(CO_2)$ measurements are important for fuel CO_2 determination. Note, that the typical measurement precision of conventional counting or AMS measurements is ±2 ‰ (equivalent to about ±1.5 µmol mol^{-1} fuel CO_2), but of the continuous GC-AMS measurements will be in the order of ±5 ‰ (equivalent to about ±3 µmol mol^{-1} fuel CO_2). The bias at $x = 0$ of about 1.1 µmol mol^{-1} is due to the insensitivity of $\Delta^{14}C(CO_2)$ against biofuel CO_2.

3.4 Measurement precision and sub-monthly variation of parameters/variables

In Sect. 3.3.1–3.3.4, we have seen how sensitive the fuel CO_2 estimates are to the total mole fractions and δ/Δ values. Since they have a large impact on the fuel CO_2 estimate, we now include their uncertainty into our analysis of precision of fuel CO_2 estimation. In order to display the effect of a limited measurement precision of CO_2, CO, $\delta^{13}C(CO_2)$ and $\Delta^{14}C(CO_2)$ we construct random realizations with mean value zero and a specific standard deviations. Additionally, we add a random sub-monthly variation to the CO offset and the biospheric/biofuel isotopic (δ/Δ-) signature in order to simulate the effect of variability of CO to CO_2 ratio and of isotopic end members. The random vectors for simulation of measurement uncertainty are y_{tot} (±0.05 µmol mol^{-1}), y_{bg} (±0.05 µmol mol^{-1}), δ_{bg} (±0.05 ‰) and δ_{meas} (±0.05 ‰), which are the typical mea-

ACPD
15, 20181–20243, 2015

surement precision of new optical instrumentation (e.g. Tuzson et al., 2011; Vardag et al., 2015). The random CO offset (±15 nmol mol^{-1}) accounts for measurement precision of total CO and of the background CO, but additionally and more importantly for natural CO sources and sinks. We have chosen the variability of 15 nmol mol^{-1}, since fuel CO_2 data from weekly-integrated $\Delta^{14}C(CO_2)$ measurements together with CO measurements indicate, that the natural CO offset typically varies within this range in Europe (Gros et al., 2002; Vogel, 2010). δ_{bio} (±2 ‰) is assumed to be a realistic variation of isotopic signature within one month (cmp. to Pataki et al., 2003). We used $\Delta^{14}C_{bio}$ (±5 ‰) (cmp. Taylor et al., 2015) and $\Delta^{14}C_{bf}$ (±10 ‰) as variation of the biospheric and biofuel $\Delta^{14}C(CO_2)$ values. $\Delta^{14}C_{bg}$ (±5 ‰) and $\Delta^{14}C_{meas}$ (±5 ‰ at hourly resolution) are assumed to be realistic measurement precisions of (potential) continuous $\Delta^{14}C(CO_2)$ measurements in near future (McIntyre et al., 2013). The sub-monthly variation of the parameters $\overline{R_F}$, $\overline{R_{tr}}$, $\overline{R_{bf}}$, $\overline{\delta_F}$, $\overline{\delta_{ff}}$, $\overline{\delta_{bf}}$, $\overline{\delta_{tr}}$, $\overline{\delta_{bio}}$, $\overline{\delta_{F\text{-}tr}}$, $\overline{m_{bf}}$ and $\overline{m_{tr}}$ is already included as we use only monthly median values of these parameters but in the STILT model these parameters vary at an hourly time scale. The distributions of the difference between estimated (incl. measurement and parameter uncertainties and sub-monthly variations) and modelled fuel CO_2 can be seen in Figs. 5–7. The finite measurement precision of mole fractions and isotope ratios considerably broaden the distributions compared to Figs. 1–3. Note that a possible misassignment of parameters or variables as investigated in Fig. 4 is neither accounted for in Figs. 1–3 nor in Figs. 5–7.

When including the measurement uncertainties and (input and footprint-weighted) parameter variability into the considerations, the distributions for rural sites (such as Gartow), medium polluted sites (such as Heidelberg) and polluted sites (such as Berlin) widen significantly by about the same amount for all three sites, due to identical assumed measurement precisions and parameter variations. Rural sites are only slightly less variable than polluted sites. However, since the absolute fuel CO_2 offset is larger in Berlin (annual modelled average ca. 25 µmol mol^{-1}), than in Heidelberg (16 µmol mol^{-1}), and in Gartow (3 µmol mol^{-1}), the relative variability (= 1σ / mean(y_F)) is smallest for the measurement site in Berlin (e.g. 14 % for $\delta^{13}C(CO_2)$-method) and

ACPD
15, 20181–20243, 2015

largest for Gartow (110 %). At present, it is therefore questionable whether the estimation of continuous fuel CO_2 is at all possible at only moderately polluted measurement sites. Even $\Delta^{14}C(CO_2)$ measurements with a precision of 5 ‰ result in a variability in fuel CO_2 of 90 % in Gartow, but a $\Delta^{14}C(CO_2)$ precision of 2 ‰ would lead to a variability in fuel CO_2 of only 35 % at rural sites (not shown here). The decrease of fuel CO_2 precision, which we observe when including limited measurement precision into our considerations, highlights again the necessity of performing precise atmospheric measurements of $\delta^{13}C(CO_2)$ and CO_2 if we want to use $\delta^{13}C(CO_2)$ as tracer for fuel CO_2.

3.5 Comparison of the estimated fuel CO_2 diurnal cycle with different tracer configurations

As the diurnal cycle of CO_2 emissions is coupled to a diurnal change of the atmospheric mixing layer height, fuel CO_2 mole fraction varies during the day. In our calculations, we only use monthly median values of $\overline{\delta_F}$, $\overline{\delta_{bio}}$, $\overline{\delta_{bf}}$, $\overline{\delta_{tr}}$, $\overline{\delta_{F\text{-}tr}}$, $\overline{\delta_{ff}}$, $\overline{R_{tr}}$, $\overline{R_{bf}}$, $\overline{R_F}$, $\overline{m_{bf}}$ and $\overline{m_{tr}}$ for fuel CO_2 estimation. Discrepancies between the modelled reference diurnal cycle and the tracer based diurnal cycle may be introduced due to a diurnal cycle of the parameters $\overline{\delta_F}$, $\overline{\delta_{bio}}$, $\overline{\delta_{bf}}$, $\overline{\delta_{tr}}$, $\overline{\delta_{F\text{-}tr}}$, $\overline{\delta_{ff}}$, $\overline{R_{tr}}$, $\overline{R_{bf}}$, $\overline{R_F}$, $\overline{m_{bf}}$ and $\overline{m_{tr}}$. We thus need to test if we are able to reproduce the diurnal fuel CO_2 pattern in order to estimate fuel CO_2 from tracers at sub-diurnal resolution. Therefore, we calculate the median diurnal fuel CO_2 cycles with the different methods and compare them to the reference model diurnal cycle for summer and for winter (see Fig. 8 exemplary for the urban station Heidelberg).

One can see that the $\delta^{13}C(CO_2)$ and the CO+ $\delta^{13}C(CO_2)$ methods reproduce the reference diurnal cycle within its variability very well (standard errors of the respective hour in a half year are denoted as error bars in Fig. 8). Median hourly differences are about $0.1 \pm 0.7\,\mu mol\,mol^{-1}$ for methods using $\delta^{13}C(CO_2)$. The CO_2-only method largely overestimates fuel CO_2 contributions during the night by up to $10\,\mu mol\,mol^{-1}$

ACPD
15, 20181–20243, 2015

in winter and by about 15–25 µmol mol^{-1} in summer. During the afternoon, the CO_2-only method overestimates fuel CO_2 in winter and underestimates it in summer. Even though the absolute difference is small during the afternoon, the relative difference is still large. The CO_2-only method is therefore not able to trace the diurnal fuel CO_2 variation at a site like Heidelberg correctly. Using $\Delta^{14}C(CO_2)$ for fuel CO_2 estimation leads to a slight median underestimation throughout the day (and season), which is due to the presence of $^{14}C(CO_2)$ in biofuel CO_2 masking all biofuel CO_2 contributions. The CO-method slightly overestimates fuel CO_2 during nighttime by about 10 % in winter and 5 % in summer. The standard deviation of the hourly medians of the differences between model and CO-based fuel CO_2 is about 6 % of the total fuel CO_2.

One could consider implementing a diurnal correction into the fuel CO_2 estimate in a way that not only monthly median values of $\overline{R_F}$, $\overline{R_{tr}}$, $\overline{R_{bf}}$, $\overline{\delta_F}$, $\overline{\delta_{ff}}$, $\overline{\delta_{bf}}$, $\overline{\delta_{tr}}$, $\overline{\delta_{bio}}$, $\overline{\delta_{F\text{-}tr}}$, $\overline{m_{bf}}$ and $\overline{m_{tr}}$ are used, but also hourly correction factors for these parameters are multiplied (cf. Vogel et al., 2010). This will be advantageous if the parameters exhibit a significant diurnal cycle themselves. However, for our setting, implementing a diurnal correction factor only weakly improves the agreement between the model and the estimated fuel CO_2 (not shown here). The reason is that the (hourly) median footprint-weighted parameters do not influence the (hourly) median fuel CO_2 estimates linearly, and that the synoptic variations of the footprint-weighted parameters are larger than the diurnal variations. Therefore, an hourly median correction factor does not necessarily improve the hourly fuel CO_2 estimate. We note that no diurnal systematic variability of the isotopic biospheric (respiration and photosynthesis) signature as well as of the natural CO sinks and sources (which would can be treated as an enhancement or reduction of the CO offset ΔCO) were implemented. Only random uncertainties of ±2 ‰ for δ_{bio} and ±15 nmol mol^{-1} for ΔCO have been implemented. This assumption of random variability will not be correct, if systematic (e.g. diurnal) variation of $\delta^{13}C_{bio}$ and natural ΔCO variation occur. For $\delta^{13}C_{bio}$ the diurnal changes are expected to be small (< 1 ‰, Flanagan et al., 2005, corresponding to y_F biases of < 0.5 µmol mol^{-1}), but for CO these may

ACPD
15, 20181–20243, 2015

be larger (e.g. diurnal natural ΔCO variation of about 10 nmol mol^{-1} may occur from dry deposition of CO in forest soils during night and from photochemical production of CO by hydrocarbons during the day (Gros et al., 2002) corresponding to ca. 2.5 µmol mol^{-1} fuel CO_2). Therefore, in a real setting, it might be necessary to model natural CO concentration in order to not introduce a bias into diurnal y_F structures.

In inverse model studies, often only afternoon hours are used to derive fluxes, as the atmospheric mixing can be better simulated by the model during conditions with a well developed mixed layer. Therefore, it is especially important to check the afternoon values of fuel CO_2. Figure 8 shows an enlarged inlay of the diurnal cycle during the afternoon hours. Since in this model study we use the minimum of total CH_4 values within two days as background value (Appendix A2), the afternoon offsets are very small, leading to a low signal to noise ratio. However, differences between the $\delta^{13}C(CO_2)$, CO, and $\Delta^{14}C(CO_2)$-based and reference fuel CO_2 are very small as well (mean differences < 10 % of afternoon fuel CO_2 value, standard deviation of differences about 30 %). Therefore, it seems justified to use the afternoon values of continuous fuel CO_2 estimates (based on $\delta^{13}C(CO_2)$ or CO) for inverse model studies despite the small absolute fuel CO_2 values of about 1–2 µmol mol^{-1} at an urban site.

4 Calibration of $\overline{\delta_F}$, $\overline{\delta_{F\text{-}tr}}$, $\overline{\delta_{ff}}$ and $\overline{R_F}$ with $\Delta^{14}C(CO_2)$ measurements

In order to estimate fuel CO_2 accurately with methods using CO and/or $\delta^{13}C(CO_2)$, the parameters $\overline{\delta_F}$, $\overline{\delta_{F\text{-}tr}}$, $\overline{\delta_{ff}}$ (and δ_{bio}) and $\overline{R_F}$ need to be known with high accuracy, since otherwise biases are introduced into the fuel CO_2 estimate (see Fig. 4). However, for the evaluation of a measured data set, $\overline{\delta_F}$, $\overline{\delta_{F\text{-}tr}}$, $\overline{\delta_{ff}}$, δ_{bio} and $\overline{R_F}$ are not available but either extensive source sampling campaigns or good bottom-up inventories are necessary. Alternatively, these parameters could also be "calibrated" using fossil fuel CO_2 estimates from $\Delta^{14}C(CO_2)$ measurements with high precision (in addition to biofuel contributions, which need to be added on top). For this purpose, Eqs. (1) and (2) can

ACPD
15, 20181–20243, 2015

be re-arranged and solved for calibration of $\overline{\delta_F}$, $\overline{\delta_{F\text{-}tr}}$, $\overline{\delta_{ff}}$ or $\overline{R_F}$ (for derivation see Appendix B). Note, that we calibrate $\overline{\delta_F}$, $\overline{\delta_{F\text{-}tr}}$, $\overline{\delta_{ff}}$ assuming a known value for $\overline{\delta_{bio}}$ (see Eqs. B1, B2 and B3). Since we use the same value of $\overline{\delta_{bio}}$ for calibration of $\overline{\delta_F}$, $\overline{\delta_{F\text{-}tr}}$, $\overline{\delta_{ff}}$ as well as for the y_F estimation (see Eqs. A7, A8 and A10), biases introduced due to a wrong $\overline{\delta_{bio}}$ cancel out. The calibration with radiocarbon measurements therefore takes care of these two unknowns at once.

Since $\Delta^{14}C(CO_2)$ measurements are time-consuming and costly, in practice only a limited number of radiocarbon measurements can be regulary performed. For example, in the Integrated Carbon Observation System (ICOS) atmospheric network, the radiocarbon measurement capacity was designed for about 50 radiocarbon measurements per station per year of which about 26 will be used for integrated sampling for long-term monitoring of fossil fuel CO_2.

Previous radiocarbon calibration approaches suggested integrated (e.g. monthly) sampling of $\Delta^{14}C(CO_2)$ for CO tracer calibration (cf. Levin and Karstens, 2007, and Vogel et al., 2010, for $\overline{R_F}$). Another possible approach for tracer calibration is to take grab samples rather than integrated samples. In the ICOS network ca. 24 radiocarbon grab samples would be available for calibration of $\overline{R_F}$ and/or $\overline{\delta_F}$, $\overline{\delta_{F\text{-}tr}}$, $\overline{\delta_{ff}}$. Grab samples could be taken through-out the year and the derived parameters $\overline{R_F}$, $\overline{\delta_F}$, $\overline{\delta_{F\text{-}tr}}$ and $\overline{\delta_{ff}}$ could then be averaged to one median value or separated into seasons and averaged to separate values e.g. for summer and winter. The optimal sampling strategy depends on the structure, variation and noise of $\overline{R_F}$, $\overline{\delta_F}$, $\overline{\delta_{F\text{-}tr}}$ and $\overline{\delta_{ff}}$ within one year. Principally, it would also be possible to take all the samples consecutively at 2 h intervals during a so-called "event" and calculate the median value from the event. Therefore, we compare here four different sampling strategies for parameter calibration, all using a total of n samples per year (in ICOS: $n \approx 24$). Note that we include sub-monthly variation into the parameters and measurement uncertainties into the observations (as in Sect. 3.4).

1. Integrated sample calibration: take $n/24$ integrated samples each month and their associated background samples ($n/24$) (for $n \approx 24$ that makes 12 monthly sam-

ACPD
15, 20181–20243, 2015

ples and 12 monthly background samples a year) and calibrate $\overline{R_F}$, $\overline{\delta_F}$, $\overline{\delta_{F\text{-}tr}}$ and $\overline{\delta_{ff}}$ on a monthly basis from the integrated samples (this corresponds to the approach suggested by Levin and Karstens, 2007, and Vogel et al., 2010, for $\overline{R_F}$). In this approach, the mean ΔCO and fuel ΔCO_2 (from integrated CO and $\Delta^{14}C(CO_2)$ sampling) over the course of one month are used to calculate monthly $\frac{\langle \Delta x \rangle}{\langle \Delta y_F \rangle}$. However, since actually the mean of ratio $\overline{R_F} = \langle \frac{\Delta x}{\Delta y_F} \rangle$ is required, and not the ratio of means $\frac{\langle \Delta x \rangle}{\langle \Delta y_F \rangle}$ (Vogel et al., 2010), biases may be introduced into the y_F estimate (same holds for the factors in $\overline{\delta_{F,F\text{-}tr,ff}}$).

2. Annual grab sample calibration: randomly select a number of samples $n/2$ (and their associated afternoon background ($n/2$)) each year and calibrate annual median $\overline{R_F}$, $\overline{\delta_F}$, $\overline{\delta_{F\text{-}tr}}$ and $\overline{\delta_{ff}}$. Biases introduced by this sampling strategy are twofold; first, the random choice of grab samples may not represent the median annual value. This potential bias decreases with the number of grab samples used. Second, the potential seasonal cycle of the parameters is not considered. Therefore, in the annual grab sample calibration, the winter-time and summer-time fuel CO_2 estimates will always be shifted against each other, as $\overline{R_F}$, $\overline{\delta_F}$, $\overline{\delta_{F\text{-}tr}}$ and $\overline{\delta_{ff}}$ exhibit a seasonal cycle, but only one annual median value for these parameters would be used.

3. Seasonal grab sample calibration: randomly select a number of samples $n/4$ (and their associated afternoon background ($n/4$)) in summer and in winter and calibrate a median $\overline{R_F}$, $\overline{\delta_F}$, $\overline{\delta_{F\text{-}tr}}$ and $\overline{\delta_{ff}}$ with half-yearly resolution. Here again, the random choice of grab samples may not represent the median annual value, but this bias is even larger here than in the annual grab sample calibration, since only half the samples are available to obtain a robust value for $\overline{R_F}$, $\overline{\delta_F}$, $\overline{\delta_{F\text{-}tr}}$ and $\overline{\delta_{ff}}$

ACPD
15, 20181–20243, 2015

for summer and winter. In return, it is principally possible to detect a seasonal variation of $\overline{R_F}$, $\overline{\delta_F}$, $\overline{\delta_{F\text{-}tr}}$ and $\overline{\delta_{ff}}$

4. Seasonal event calibration: randomly select an "event day" each season. On this day, select $n/2 - 2$ consecutive grab samples (and 1 associated afternoon background) and calibrate a median $\overline{R_F}$, $\overline{\delta_F}$, $\overline{\delta_{F\text{-}tr}}$ and $\overline{\delta_{ff}}$ with half-yearly resolution. This approach is similar to approach 3, but entails a greater risk of choosing an event, which is not representative for the entire season, since subsequent samples are not independent of each other. On the other side, it has the advantage of using more calibrations for the same amount of radiocarbon measurements as approach 3 since only one background sample is needed for each event.

Comparing these sampling strategies to each other using one model run is difficult, since the result changes from random realization to random realization depending on the selection of calibration samples in sampling strategy 2–4. We have therefore performed 5000 model runs, and used the root median square difference between the obtained and originally modelled reference values $\overline{R_F}$, $\overline{\delta_F}$, $\overline{\delta_{F\text{-}tr}}$ and $\overline{\delta_{ff}}$ to calculate the difference between tracer-based estimate and modelled reference fuel CO_2.

Table 3 shows the mean difference and standard deviation (as determined from a Gaussian fit to the difference histogram of modelled and tracer-based fuel CO_2, in analogy to Fig. 5) for an urban setting. One can see that the "integrated sample calibration" causes biases due to the covariance of the factors in Eqs. (B1)–(B4). The effect is much stronger for methods using $\delta^{13}C(CO_2)$ (ca. 15 % of mean fuel CO_2 offset in Heidelberg (16 µmol mol^{-1}) than for the CO method (ca. 8 %). Thus, it seems that integrated sampling of $\Delta^{14}C(CO_2)$, although important for long-term monitoring of fuel CO_2, cannot be reliably used in addition for calibration of continuous fuel CO_2 estimating methods. Note, that the differences found here are not due to the insensitivity of biofuel CO_2 contributions of $\Delta^{14}C(CO_2)$, as we add the (assumed as known) biofuel CO_2 prior to "calibration" (see Eqs. B1–B3).

ACPD
15, 20181–20243, 2015

We further find that since $\overline{\delta_F}$, $\overline{\delta_{F\text{-}tr}}$, $\overline{\delta_{ff}}$ and $\overline{R_F}$ do not exhibit a strong annual cycle, but show rather large, high-frequent variations, the best sampling strategy for 24 available radiocarbon measurements per year (as would be the case for the ICOS network) is, using all available samples to calibrate well-defined median annual values of $\overline{R_F}$, $\overline{\delta_F}$, $\overline{\delta_{F\text{-}tr}}$ and $\overline{\delta_{ff}}$ (sampling strategy 2). Only, when using the $\delta^{13}C(CO_2)$ method with 96 (or more) available radiocarbon measurements, it is advisable to group the calibrations into half-yearly median intervals. This may be a realistic scenario, if the parameter $\overline{\delta_F}$ does not show any trend over the course of various years.

The accuracy of the seasonal event calibration is very similar to the accuracy of the seasonal calibration, but slightly better for 24 available radiocarbon samples (see Table 3) since more calibrations per radiocarbon samples are available. It is slightly worse for 96 samples due to non-representativeness of a single event for the entire season.

5 Discussion

In this work, we analyzed the advantages and disadvantages of different tracers for estimating continuous fuel CO_2 at different types of measurement stations. We calculate the accuracy and precision of continuous fuel CO_2 at three exemplary stations; one rural, one urban and one polluted station. This should serve as orientation for the development of an atmospheric measurement strategy, so that the best tracer configuration for a particular station can be chosen to resolve the different CO_2 source components over a country or region. The results can be used to plan and construct new measurement networks and sampling strategies with the goal of deriving fuel CO_2 concentrations on high temporal resolution. In order to improve inverse model approaches, tracer-based continuous fuel CO_2 estimates should be more accurate and precise than those derived from bottom-up inventories with uncertainties of 30–150 % at regional resolution (Wang et al., 2013). We therefore seek to monitor continuous fuel CO_2 with

ACPD
15, 20181–20243, 2015

a precision of at least 30 % and with biases smaller than 10 %. In the discussion, we focus on the results obtained when including the currently achievable measurement uncertainty into the tracer records (see Figs. 5–7 and Table 3). If measurement precision improves further, the precision of the fuel estimate will also increase and approach the upper limit of accuracy and precision (Figs. 1–3) if δ_i and R_i are perfectly well known.

5.1 Evaluation of the CO_2-only method

The simplest approach is to use total CO_2 as a proxy for fuel CO_2. However, as soon as CO_2 is released or taken up by the biosphere, total CO_2 will not be an adequate tracer for fuel CO_2. For all stations investigated, we found that biogenic CO_2 contributions are generally not negligible and vary on the time scale of hours. Only during the winter time in strongly polluted areas, biogenic CO_2 contributions lead to a relatively small bias of about 5 % and show small variation (σ / mean(y_F): 5 %, see Fig. 7). For stations with more biospheric activity in the catchment area, total CO_2 significantly overestimated fuel CO_2 and leads to strong variations. Therefore, other fuel CO_2 tracers need to be considered in these cases.

5.2 Evaluation of the CO and $\delta^{13}C(CO_2)$ methods

The accuracy of CO and/or $\delta^{13}C(CO_2)$ based fuel CO_2 estimates depends to a large degree on how well the different parameters such as $\overline{R_F}$, $\overline{R_{tr}}$, $\overline{R_{bf}}$, $\overline{\delta_F}$, $\overline{\delta_{ff}}$, $\overline{\delta_{bf}}$, $\overline{\delta_{tr}}$, $\overline{\delta_{F\text{-}tr}}$, $\overline{m_{bf}}$, $\overline{m_{tr}}$ and δ_{bio} are known. If the monthly median values of these parameters are perfectly well known, methods using $\delta^{13}C(CO_2)$ or CO are very accurate for all measurement sites (see Figs. 1–3b–e and 5–7b–e). However, misassignment of some parameters, e.g. the mean isotopic signatures $\overline{\delta_{ff}}$, $\overline{\delta_{bf}}$, $\overline{\delta_{tr}}$, $\overline{\delta_{F\text{-}tr}}$ and δ_{bio} leads to a significant bias in the fossil fuel CO_2 estimate (Fig. 4). Therefore, in practice, it is important to screen and monitor all sources and sinks in the catchment area of the measurement site and to determine the median isotopic source signature and the median ratios $\overline{R_F}$, $\overline{R_{tr}}$, $\overline{R_{bf}}$ or the CO offset as accurately as possible, e.g. by calibration with co-located

ACPD
15, 20181–20243, 2015

$\Delta^{14}C(CO_2)$ measurements. However, a calibration using integrated $\Delta^{14}C(CO_2)$ samples is not feasible without introducing biases (see Table 3). It is preferable to use $\Delta^{14}C(CO_2)$ grab samples for calibration of $\overline{R_F}$, $\overline{R_{tr}}$, $\overline{R_{bf}}$, $\overline{\delta_F}$, $\overline{\delta_{ff}}$, $\overline{\delta_{bf}}$, $\overline{\delta_{tr}}$ or $\overline{\delta_{F\text{-}tr}}$. We found that the accuracy of the $\overline{R_F}$, $\overline{R_{tr}}$, $\overline{R_{bf}}$, $\overline{\delta_F}$, $\overline{\delta_{ff}}$, $\overline{\delta_{bf}}$, $\overline{\delta_{tr}}$ or $\overline{\delta_{F\text{-}tr}}$ determination depends on the number of radiocarbon samples available and on the sampling strategy used. In the ICOS project approximately 24 radiocarbon samples will be available for calibration of $\overline{R_F}$, $\overline{\delta_F}$, $\overline{\delta_{ff}}$, $\overline{\delta_{bf}}$, $\overline{\delta_{tr}}$ or $\overline{\delta_{F\text{-}tr}}$. For that amount of calibration samples available, we find that due to the large noise of the calibrated footprint-weighted parameters $\overline{R_F}$, $\overline{\delta_F}$, $\overline{\delta_{ff}}$, $\overline{\delta_{bf}}$, $\overline{\delta_{tr}}$ or $\overline{\delta_{F\text{-}tr}}$ it is advantageous to group all calibrations to obtain robust annual median values for $\overline{R_F}$, $\overline{\delta_F}$, $\overline{\delta_{ff}}$, $\overline{\delta_{bf}}$, $\overline{\delta_{tr}}$ or $\overline{\delta_{F\text{-}tr}}$. In this case, the accuracy will typically be better than 10 % when using the CO-method or the $\delta^{13}C(CO_2)$ method. Only if a large number of precise radiocarbon measurements are available or if the parameters do not change over the course of several years and thus, several years of calibration samples can be accumulated, it is advantageous to apply radiocarbon calibrations at half-yearly resolution. Note, that due to changes in technology and technical processes, as well as due to a year-to-year variation of extreme temperatures, the weight of the different sectors is likely to change within a period of four years. However, this could be checked using night-time Keeling plot intercepts.

CO as fuel CO_2 tracer shows a precision (e.g. 1σ / mean(y_F)) of about 30–40 % for Heidelberg. The uncertainty originates mainly from the large variation of $\overline{R_F}$ in our model runs due to the inhomogeneity of fuel CO sources in the footprint area of urban or polluted measurement stations and due to natural CO sources. For the rural station of Gartow, the precision of the CO-based approach is comparable to the precision of the $\delta^{13}C(CO_2)$ -based approach, but for urban or polluted areas the precision of the $\delta^{13}C(CO_2)$-based approach seems more promising.

The uncertainty of the $\delta^{13}C(CO_2)$ approach (e.g. 1σ / mean(y_F) $\approx$ 30 % for Heidelberg) is mainly determined by the limited measurement precision of $\delta^{13}C(CO_2)$. Thus

ACPD
15, 20181–20243, 2015

in order to use $\delta^{13}C(CO_2)$ as a tracer for fuel CO_2 it is vital to perform isotopic measurements with a measurement precision of at least 0.05 ‰. The combination of $\delta^{13}C(CO_2)$ and CO for fuel CO_2 estimation is favorable in cases where each of two emission groups is well distinguishable by one of the tracers. Since for our model setting this is only partly the case (EDGAR emission inventory, see Table A1), the combination of these tracers provides only little additional information.

When evaluating CO or $\delta^{13}C(CO_2)$ as tracer for fuel CO_2, one should keep in mind that the precision of approaches using $\delta^{13}C(CO_2)$ and CO depend also on the source characteristics in the catchment area. For example, $\delta^{13}C(CO_2)$ is especially qualified as a tracer for fuel CO_2 when all fuel CO_2 sources in the catchment area of the measurement site are strongly depleted compared to biospheric CO_2 (see Appendix, Fig. A1). The source characteristics in the catchment area of a measurement site must therefore be considered when estimating the precision of fuel CO_2 at a particular station.

5.3 Evaluation of $\Delta^{14}C(CO_2)$ method

We have found, that $\Delta^{14}C(CO_2)$ measurements with 5 ‰ precision (see Figs. 5–7) would generally be the most precise tracer for continuous fuel CO_2 estimation at rural (1σ / mean(y_F) ≈ 90 %), urban (ca. 20 %) and polluted (ca. 10 %) stations. The precision of fuel CO_2 estimates is determined mainly by the limited measurement precision of background and total $\Delta^{14}C(CO_2)$ (±5‰). Note however, that $\Delta^{14}C(CO_2)$ measurements with 5 ‰ precision are not yet fully developed and commercially available. The downside of $\Delta^{14}C(CO_2)$ is its inability to determine biofuel CO_2. Therefore, the $\Delta^{14}C(CO_2)$ methods will underestimate the fuel CO_2 (biofuel plus fossil fuel) contributions approximately by the share of biofuel in CO_2 at the site. This may be only a small contribution as was the case for the studied year 2012 (e.g. 5 % in Heidelberg), but may increase in the future. Therefore, for an unbiased estimation of fuel CO_2 using $\Delta^{14}C(CO_2)$, biofuel CO_2 would need to be added individually, e.g. using the tracer CO

ACPD
15, 20181–20243, 2015

or from bottom-up inventories. For some purposes, it may actually be advantageous to estimate only the fossil fuel CO_2 contribution, which is the fuel CO_2 contribution without biofuel CO_2 and therefore excludes short-cycle carbon. However, for model inversions, the biofuel CO_2 is important as well, since it equally contributes to the instantaneous measured CO_2 concentration.

So far, we have not investigated the effect of nuclear power plant $^{14}C(CO_2)$ contributions at the measurement site, which could additionally bias fuel CO_2 estimates derived from $\Delta^{14}C(CO_2)$ measurements. Dispersion model results for Heidelberg (M. Kuderer, personal communication, 2015) suggest that the nuclear power facilities (most importantly Philippsburg, located about 25 km south-west of Heidelberg), increase monthly mean $\Delta^{14}C(CO_2)$ by about 2 ± 2 ‰, corresponding to a misassignment in fuel CO_2 of about $0.8 \pm 0.8\,\mu mol\,mol^{-1}$ (≈ 5 %). If there are nuclear power plants or fuel reprocessing plants in the catchment area of the measurement site and if monthly mean emission data of pure $^{14}C(CO_2)$ from these nuclear power plants are available, it is advisable to correct for them at the highest possible temporal resolution e.g. using transport models (Vogel et al., 2013b). Note, that for the calibration of $\overline{R_F}$, $\overline{\delta_F}$, $\overline{\delta_{ff}}$, $\overline{\delta_{bf}}$, $\overline{\delta_{tr}}$ or $\overline{\delta_{F\text{-}tr}}$ using $\Delta^{14}C(CO_2)$ grab samples, it should be possible to choose the calibration grab samples via trajectory forecast such that no nuclear power plant influences are encountered in the grab samples.

5.4 Relative precision at different measurement sites

When comparing the precision of the CO, $\delta^{13}C(CO_2)$ and $\Delta^{14}C(CO_2)$ tracer methods at the rural, urban and polluted model station, we find that rural sites seem to exhibit similar, but slightly smaller variations. However, since the mean fuel CO_2 offset is larger at more polluted measurement sites, the relative precision is much better there and different tracer configurations for monitoring fuel CO_2 seem much more promising at polluted locations. Due to the small fuel CO_2 offsets at rural sites, it does not seem feasible, at present state, to monitor continuous fuel CO_2 with sufficient precision with

ACPD
15, 20181–20243, 2015

any of the tracers explored here. This may be important to consider when planning fuel CO_2 monitoring in national or international measurement networks.

5.5 Evaluation of diurnal biases in fuel CO_2

We have compared the diurnal cycle of the fossil fuel estimates using the different tracers. For Heidelberg, we found that the tracer configurations using CO, $\delta^{13}C(CO_2)$ and $\Delta^{14}C(CO_2)$ were able to reproduce the diurnal cycle well within 5 % (1σ). This may be surprising, since one might expect a diurnal pattern of $\overline{\delta_F}$ and $\overline{R_F}$ due to a varying share of emissions of different emission sectors in the footprint, leading to a systematic deviation of the estimated from the real modelled diurnal cycle. However, since the diurnal patterns are small (peak to peak difference of $\overline{\delta_F}$ ca. 2 ‰), the mean diurnal variations are not significantly improved when using a diurnal correction of the mean isotopic source signatures. One should keep in mind that natural CO contributions may also vary systematically on a diurnal basis. A systematic variation was not included into the model simulation, but will potentially introduce a diurnal bias into the continuous fuel CO_2 estimate in a real setting. Therefore, it may be necessary to model or approximate natural CO in a real setting. It may be possible to approximate the (sub-monthly) natural CO component using formaldehyde (HCHO) measurements, since the production of CO from NMHC pass HCHO as intermediate molecule (Atkinson, 2000). However, the high dry deposition rate of HCHO may complicate the interpretation further. Since afternoon values are often used in inverse model studies to derive fluxes it is important, that afternoon fuel CO_2 values can be estimated accurately. This could be confirmed for $\delta^{13}C(CO_2)$ and CO in this study (see Fig. 8).

6 Conclusion

The results of our model study suggest that with our current measurement precision of continuous tracers such as CO, $\delta^{13}C(CO_2)$ or $\Delta^{14}C(CO_2)$, it is not possible to estimate

ACPD
15, 20181–20243, 2015

fuel CO_2 at rural areas with a precision better than 90 %. Therefore, the design of some atmospheric measurement networks such as that of ICOS, may need to be revised if fuel CO_2 contributions shall be monitored and evaluated. At present, it seems not helpful to equip measurement stations in rural areas with instruments for $\delta^{13}C(CO_2)$ and CO measurements with the objective of monitoring continuous fuel CO_2. However, installation of instruments measuring these components at urban or polluted sites (as e.g. planned within the Megacities Carbon project) seems worthwhile in order to improve the fuel CO_2 bottom-up inventories.

Potential future continuous $\Delta^{14}C(CO_2)$ measurement with a precision of 5 ‰ is the most promising tracer (precision ca. 10–20 %), but the insensitivity against biofuel contributions as well as nuclear power plant emissions of $^{14}C(CO_2)$ need to be considered. $\delta^{13}C(CO_2)$ and CO-based methods do not suffer from these shortcomings, but require accurate characterization (e.g. via precise radiocarbon measurements) of the sources in the catchment area of the measurement site with respect to $\overline{R_F}$, $\overline{R_{tr}}$, $\overline{R_{bf}}$, $\overline{\delta_F}$, $\overline{\delta_{ff}}$, $\overline{\delta_{bf}}$, $\overline{\delta_{tr}}$ or $\overline{\delta_{F\text{-}tr}}$. For a limited number (e.g. 24) of precise $\Delta^{14}C(CO_2)$ measurements available, the best sampling strategy is to calibrate the footprint-weighted parameters using grab samples and averaging all to obtain median annual footprint-weighted parameters $\overline{R_F}$, $\overline{R_{tr}}$, $\overline{R_{bf}}$, $\overline{\delta_F}$, $\overline{\delta_{ff}}$, $\overline{\delta_{bf}}$, $\overline{\delta_{tr}}$ and $\overline{\delta_{F\text{-}tr}}$. Typically, we can then obtain fuel CO_2 estimates with a bias of about 10 % and a precision of 25–40 %. This is smaller than the uncertainties of bottom-up inventories and therefore opens the door for a significant improvement of highly resolved emission inventories from atmospheric observation. The precision of the $\delta^{13}C(CO_2)$ method may further increase in future, if the measurement precision of $\delta^{13}C(CO_2)$ improves.

ACPD
15, 20181–20243, 2015

Appendix A: Methods of continuous fuel CO_2 determination

A1 Tracer configurations and their emission groups

We formally introduce six different tracers or tracer combinations, which we use to estimate fuel CO_2 continuously: CO_2 is used as sole tracer for fuel CO_2. CO, $\delta^{13}C(CO_2)$ and $\Delta^{14}C(CO_2)$ records are each used solely with CO_2 to estimate fuel CO_2. Further, CO is used as tracer for traffic (and $\delta^{13}C(CO_2)$ as tracer for fuel CO_2 minus traffic) and finally CO is used as tracer for biofuels (and $\delta^{13}C(CO_2)$ as tracer for fuel CO_2 minus biofuels). The different emission groups are also listed and characterized in Table A1.

A1.1 CO_2 as sole tracer for fuel CO_2

When using CO_2 alone as "tracer" for fuel CO_2 ($y_F = y_{ff} + y_{bf}$), the total regional CO_2 offset is assumed to solely originate from fuel emissions:

$$y_F = \Delta y \tag{A1}$$

With $\Delta y = y_{tot} - y_{bg}$.

This simple approach is valid, if (nearly) all CO_2 emissions are from fuel burning, as might be the case in cold winters or in areas without biospheric activity (e.g. Mega cities).

A1.2 CO as tracer for fuel CO_2

The CO offset ($\Delta x = x_{tot} - x_{bg}$) can be used to estimate fuel CO_2 offset if it is divided by the mean ratio $\overline{R_F} = \Delta x \,/\, \Delta y_F$ of all fuel sources:

$$y_F = \frac{\Delta x}{\overline{R_F}} \tag{A2}$$

ACPD
15, 20181–20243, 2015

Note that in reality the ratio $\overline{R_F}$ varies, depending on the share of emissions of different emission sectors in the catchment area, their temporal emission patterns, and due to natural CO sources and sinks, at least in summer (Prather et al., 2001). We denote $\overline{R_F}$ with an overbar to emphasize that this is a footprint-weighted average of the fuel emission ratio.

A1.3 CO as tracer for traffic CO_2 and $\delta^{13}C(CO_2)$ as tracer for all fuel CO_2, except for traffic CO_2

We now include $\delta^{13}C(CO_2)$ in fuel CO_2 estimation as a tracer for all fuel CO_2 except those of traffic ($y_{F\text{-}tr} = y_{ff} + y_{bf} - y_{tr}$).

$$y_{tot} = y_{bg} + y_{bio} + y_{tr} + y_{F\text{-}tr} \tag{A3}$$

$$y_{tot}\delta_{tot} = y_{bg}\delta_{bg} + y_{bio}\delta_{bio} + y_{tr}\overline{\delta_{tr}} + y_{F\text{-}tr}\overline{\delta_{F\text{-}tr}} \tag{A4}$$

In analogy to $\overline{R_F}$ we denote $\overline{\delta_{tr}}$ and $\overline{\delta_{F\text{-}tr}}$ with an overbar to emphasize that these are footprint-weighted averages of the emission groups traffic CO_2 and fuel CO_2 excluding traffic, respectively. Solving Eq. (A3) for y_{bio}, we can substitute y_{bio} in Eq. (A4). In analogy to Eq. (A2), we use CO as tracer for traffic CO_2:

$$y_{tr}(t) = \frac{x_{tr}(t)}{\overline{R_{tr}}} \tag{A5}$$

With the mean $\Delta CO / \Delta CO_2$ ratio of traffic $\overline{R_{tr}} = (\Delta x / \Delta y)_{tr}$. CO_{tr} can be determined from:

$$CO_{tr}(t) = \Delta CO(t) \cdot \overline{m_{tr}} \tag{A6}$$

with $\overline{m_{tr}} = (\Delta x_{tr} / \Delta x)$ being the share of traffic CO to the total CO offset. $\overline{m_{tr}}$ needs to be estimated from bottom-up inventories and can be found in Table A1 (right column)

ACPD
15, 20181–20243, 2015

and is also dependent on the footprint area of the measurement site and the sources and sinks lying in this area. Equations (A3)–(A6) can then be re-arranged:

$$y_{\text{F-tr}} = \frac{y_{\text{tot}}\delta_{\text{tot}} - y_{\text{bg}}\delta_{\text{bg}} - \left(y_{\text{tot}} - y_{\text{bg}} - y_{\text{tr}}\right)\delta_{\text{bio}} - y_{\text{tr}}\overline{\delta_{\text{tr}}}}{\overline{\delta_{\text{F-tr}}} - \delta_{\text{bio}}} \tag{A7}$$

Total fuel CO_2 (y_F) contribution can then be determined as the sum of y_{tr} (Eq. A5) and $y_{\text{F-tr}}$ (Eq. A7).

A1.4 CO as tracer for biofuel CO_2 and $\delta^{13}C(CO_2)$ as tracer for all fuel CO_2, except for biofuel CO_2

This method of fuel CO_2 estimation is in analogy to Sect. A.1.3, but instead of separating fuel CO_2 in to traffic contributions (y_{tr}) and others ($y_{\text{F-tr}}$), we separate it into biofuel contributions (y_{bf}) and others ($y_{\text{F-bf}} = y_{\text{ff}}$); this leads to:

$$y_{\text{F-bf}} = \frac{y_{\text{tot}}\delta_{\text{tot}} - y_{\text{bg}}\delta_{\text{bg}} - (y_{\text{tot}} - y_{\text{bg}} - y_{\text{bf}})\delta_{\text{bio}} - y_{\text{bf}}\overline{\delta_{\text{bf}}}}{\overline{\delta_{\text{ff}}} - \delta_{\text{bio}}} \tag{A8}$$

Analogously to Eq. (A10), we formulate for y_{bf}:

$$y_{\text{bf}}(t) = \frac{\Delta x(t) \cdot \overline{m_{\text{bf}}}}{\overline{R_{\text{bf}}}} \tag{A9}$$

With $\overline{m_{\text{bf}}} = (\Delta x_{\text{bf}} / \Delta x)$ from bottom-up inventories (see Table A1). Total fuel CO_2 (y_F) is calculated as the sum of y_{bf} (Eq. A9) and $y_{\text{F-bf}}$ (Eq. A9).

ACPD
15, 20181–20243, 2015

A1.5 $\delta^{13}C(CO_2)$ as sole tracer for fuel emission

When using δ_{tot} as tracer for all fuel contributions, Eqs. (A3) and (A4) simplify to

$$y_F = \frac{y_{tot}\delta_{tot} - y_{bg}\delta_{bg} - (y_{tot} - y_{bg})\delta_{bio}}{\overline{\delta_F} - \delta_{bio}} \quad \text{(A10)}$$

if all fuel CO_2 ($y_{F\text{-}tr}$ and y_{tr}) contributions are pooled to y_F.

A1.6 $\Delta^{14}C(CO_2)$ as tracer for fossil fuel CO_2

Following Levin et al. (2008), we can derive fossil fuel CO_2 from $\Delta^{14}C(CO_2)$ and total CO_2 measurements according to:

$$y_{ff} = \frac{y_{bg}\left(\Delta^{14}C_{bg} - \Delta^{14}C_{bio}\right) - y_{tot}\left(\Delta^{14}C_{tot} - \Delta^{14}C_{bio}\right) - y_{bf}\left(\Delta^{14}C_{bio} - \Delta^{14}C_{bf}\right)}{1 + \Delta^{14}C_{bio}} \quad \text{(A11)}$$

However, since $\Delta^{14}C_{bio} \approx \Delta^{14}C_{bf}$, and because biofuel contributions are not known, we neglect the last term of the numerator in the following. Note, that since $\Delta^{14}C(CO_2)$ is not sensitive to biofuel contributions, it is only possible to estimate the fossil fuel CO_2 contributions without biofuel contributions.

A2 Determination of parameters and variables

The background values y_{bg}, x_{bg}, δ_{bg} and $\Delta^{14}C_{bg}$ should represent the regional clean air to which the source contributions from the footprint area are added. Since often, there are no nearby clean-air observations available for a polluted station, we use those mole fractions as background where the air masses in the boundary layer are well mixed with the free troposphere. This is usually the case in the afternoon and is associated with

ACPD
15, 20181–20243, 2015

low mole fractions. Since CO_2, as well as CO both have local sinks relevant on the timescale of days, we here use CH_4 as an indicator for a well-mixed boundary layer and assume that, when the CH_4 mole fraction reaches a minimum value (within two days), vertical mixing is strongest. Principally, if continuous radon measurements were available, these could also be used as an indicator for vertical mixing (Dörr et al., 1983), instead of CH_4. We checked that the CH_4 minimum values always represent a lower envelope of the simulated greenhouse gas record and does not vary at the synoptic time scale. We then use the total mole fractions and isotopic records y_{tot}, x_{tot}, δ_{tot}, and $\Delta^{14}C_{tot}$ observed during situations with minimal CH_4 mole fractions as background values.

Further, in order to solve Eqs. (A2)–(A11), we need the input parameters δ_{bio}, $\Delta^{14}C_{bio}$. These input parameters were assigned with the objective to create realistic modelled data set (see Tables 1 and A1). Additionally, the integrated footprint-weighted parameters $\overline{R_F}$, $\overline{R_{tr}}$, $\overline{R_{bf}}$, $\overline{\delta_F}$, $\overline{\delta_{ff}}$, $\overline{\delta_{bf}}$, $\overline{\delta_{tr}}$, $\overline{\delta_{bio}}$, $\overline{\delta_{F\text{-}tr}}$, $\overline{m_{bf}}$ and $\overline{m_{tr}}$ are required (see Table A1). We call these parameters footprint-weighted, since the ratios and isotopic signatures depend on the relative contribution from the different emission sectors (with their sector specific emission ratios and isotopic signatures) within the footprint of the measurement site. We denote the integrated footprint-weighted parameters with an overbar to draw attention to the fact that the parameters are averaged over the (e.g. monthly) footprint area. Even though the emission factors of the source categories used here are fixed for every pixel, integrated footprint-weighted $\overline{R_F}$, $\overline{R_{tr}}$, $\overline{R_{bf}}$, $\overline{\delta_F}$, $\overline{\delta_{ff}}$, $\overline{\delta_{bf}}$, $\overline{\delta_{tr}}$, $\overline{\delta_{bio}}$, $\overline{\delta_{F\text{-}tr}}$, $\overline{m_{bf}}$ and $\overline{m_{tr}}$ are not constant in time, because the footprint of the measurement site and the emission patterns are temporally variable. Thus, the footprint-weighted parameters change when the emissions from the different sectors or the footprint of the measurement site vary. Note, that for our model study we do not require the parameters to be absolutely correct, since we do not compare them to measured data. However, since we want to provide a realistic case study, we seek to use the most realistic parameters (see values in Tables 1 and A1).

ACPD
15, 20181–20243, 2015

Appendix B: "Calibration" with $\Delta^{14}C(CO_2)$

Solving Eqs. (A3), (A8), (A9) and (A11) for fuel CO_2 requires $\overline{R_F}$, $\overline{\delta_F}$, $\overline{\delta_{ff}}$ and $\overline{\delta_{F\text{-}tr}}$. If these values are not known, they may be derived from $\Delta^{14}C(CO_2)$ observations (what we then call $\Delta^{14}C(CO_2)$-calibrated). However, for the calibration y_{ff} must be known. The idea is to calibrate fossil fuel CO_2, e.g. with precise $\Delta^{14}C(CO_2)$ measurements, on a lower time resolution (e.g. monthly) and assume that the footprint-weighted parameters $\overline{R_F}$, $\overline{\delta_F}$ $\overline{\delta_{ff}}$ and $\overline{\delta_{F\text{-}tr}}$ do not change significantly within this calibration interval.

Re-arranging Eqs. (1) and (2) for $\overline{\delta_{ff}}$ and averaging it monthly leads to

$$\overline{\delta_{ff}} = \frac{y_{tot}\delta_{tot} - y_{bg}\delta_{bg} - (y_{tot} - y_{bg} - y_{ff} - y_{bf})\delta_{bio} - y_{bf}\overline{\delta_{bf}}}{y_{ff}}, \tag{B1}$$

which could then be used in Eq. (A9). Note that we require the biofuel CO_2 in addition to the fossil fuel CO_2 from $\Delta^{14}C(CO_2)$.

$\overline{\delta_F}$ can then be derived, if the y_{bf} concentration is known.

$$\overline{\delta_F} = \frac{\overline{\delta_{ff}}y_{ff} + \overline{\delta_{bf}}y_{bf}}{y_{ff} + y_{bf}} \tag{B2}$$

If fossil fuel emissions are divided into fossil fuel contributions without traffic ($y_{F\text{-}tr}$) and traffic contributions (y_{tr}), we can derive $\overline{\delta_{F\text{-}tr}}$ required for solving Eq. (A8):

$$\overline{\delta_{F\text{-}tr}} = \frac{\overline{\delta_F}y_F - \overline{\delta_{tr}}y_{tr}}{y_F - y_{tr}} \tag{B3}$$

Analogously, the ratio $\overline{R_F}$ could be calibrated following:

$$\overline{R_F} = \frac{\Delta x}{\Delta y_F} \tag{B4}$$

ACPD
15, 20181–20243, 2015

In order to calculate the monthly mean value of $\langle\overline{\delta_F}\rangle$ and $\langle\overline{R_F}\rangle$, the mean ratios $\langle\frac{\Delta x}{\Delta y_F}\rangle$ (Eqs. B1–B4) are needed. However, from integrated $\Delta^{14}C(CO_2)$ sampling, we only have the mean fossil fuel CO_2 and fuel CO_2 values and can thus, only calculate $\frac{\langle\Delta x\rangle}{\langle\Delta y_F\rangle}$. Using the product (or ratio) of the means rather than the mean of the product (ratio) is only correct if the factors are uncorrelated. Since, the factors in Eqs. (B1)–(B4) (and Δx and Δy_{ff}) are correlated, the integrated calibration cannot be applied without introducing a bias into monthly mean $\langle\overline{\delta_F}\rangle$, $\langle\overline{\delta_{ff}}\rangle$, $\langle\overline{\delta_{F\text{-}tr}}\rangle$ and $\langle\overline{R_F}\rangle$. Instead of using integrated $\Delta^{14}C(CO_2)$ samples in order to obtain the monthly fossil fuel CO_2 values, it is possible to take grab samples, analyse these for $\Delta^{14}C(CO_2)$ (and with that y_{ff}), total CO_2, $\delta^{13}C(CO_2)_{tot}$ and CO in order to calculate the individual (non-averaged) values for $\overline{\delta_F}$, $\overline{\delta_{F\text{-}tr}}$, $\overline{\delta_{ff}}$ and $\overline{R_F}$ (see Sect. 4).

Appendix C: Influence of more depleted fuel $\delta^{13}C(CO_2)$ signatures

We have argued that we only require a realistic set of input parameters, rather than an absolutely correct set of parameters to estimate uncertainties of the different tracer methods. However, the results presented so far are to some degree dependent on the emission characteristics used in our model (see Table A1). When using CO as tracer for fuel CO_2, it would be advantageous if natural sources of CO were negligible and if the emission ratio $\overline{R_F}$ would be the same for all sources. When using CO_2 as tracer for fuel CO_2, biospheric CO_2 emissions should be negligible, and when using $\delta^{13}C(CO_2)$, it would be advantageous if fuel CO_2 emissions were strongly depleted compared to biospheric emissions. It is beyond the scope of this work, to show explicitly for all cases how the "choice" of different emission characteristics influences the fuel CO_2 estimate in terms of precision and accuracy. However, in Fig. A1, we illustrate exemplary for this latter case how the presence of more depleted fuel sources in the footprint area of the measurement site could improve the tracer $\delta^{13}C(CO_2)$ for fuel CO_2 estimation. This

ACPD
15, 20181–20243, 2015

should serve as an example, showing how much the emission characteristics at a site may influence the precision of fuel CO_2 estimates using different tracer configurations.

Figure A1 shows that fuel CO_2 can be estimated much better when the mean source mix in the catchment area of the measurement site exhibits a strongly depleted isotopic source signature. The regression coefficient improves from 0.94 to 0.99 and the precision within one year decreases significantly by 40 % when choosing $\overline{\delta_F}$ 7 ‰ more depleted (−39 ‰ instead of −32 ‰). The precision of $\delta^{13}C(CO_2)$-based fuel CO_2 will increase with decreasing isotopic signature of fuel CO_2 sources. Analogously, the precision of CO-based fuel CO_2 estimates will increase with decreasing inhomogeneity of CO / CO_2 ratio of fuel CO_2 sources. This effect should be taken into account when designing a measurement network and thus highlights the importance of a thorough source evaluation in the catchment area prior to instrumental installation.

Acknowledgements. We thank Ute Karstens and Thomas Koch for valuable modelling lessons and help with setting up the model. We are also thankful for valuable discussions on fossil fuel CO_2 in Heidelberg with Felix R. Vogel and Samuel Hammer. This work has been funded by the InGOS EU project (284274) and ICOS BMBF project (01LK1225A).

References

Ahmadov, R., Gerbig, C., Kretschmer, R., Koerner, S., Neininger, B., Dolman, A. J., and Sarrat, C.: Mesoscale covariance of transport and CO_2 fluxes: Evidence from observations and simulations using the WRF-VPRM coupled atmosphere-biosphere model, J. Geophys. Res., 112, D22107, doi:10.1029/2007JD008552, 2007.

Atkinson, R.: Atmospheric chemistry of VOCs and NO_x, Atmos. Environ., 34, 2063–2101, 2000.

Ballantyne, A. P., Miller, J. B., Baker, I. T., Tans, P. P., and White, J. W. C.: Novel applications of carbon isotopes in atmospheric CO_2: what can atmospheric measurements teach us about processes in the biosphere?, Biogeosciences, 8, 3093–3106, doi:10.5194/bg-8-3093-2011, 2011.

ACPD
15, 20181–20243, 2015

Bousquet, P., Peylin, P., Ciais, P., Le Quéré, C., Friedlingstein, P., and Tans, P. P.: Regional changes in carbon dioxide fluxes of land and oceans since 1980, Science, 290, 1342–1346, 2000.

BP: The role of biofuels beyond 2020, Technical report issued September 2013, available at: http://www.bp.com/en/global/alternative-energy/our-businesses/biofuels.html, last access: 23 February 2015.

Conrad, R.: Soil microorganisms as controllers of atmospheric trace gases (H_2, CO, CH_4, OCS, N_2O, and NO), Microbiol. Rev., 60, 609–640, 1996.

Coyle, W.: The future of biofuels, Economic Research Service, Washington, DC, 2007.

Denier van der Gon, H. D., Hendriks, C., Kuenen, J., Segers, A., and Visschedijk, A.: Description of current temporal emission patterns and sensitivity of predicted AQ for temporal emission patterns, TNP Report, EU FP7 MACC deliverable report D_D-EMIS_1.3., available at: https://gmes-atmosphere.eu/documents/deliverables/d-emis/MACC_TNO_del_1_3_v2.pdf (last access: 22 July 2015), 2011.

Djuricin, S., Pataki, D. E., and Xu, X.: A comparison of tracer methods for quantifying CO_2 sources in an urban region, J. Geophys. Res., 115, D11303, doi:10.1029/2009JD012236, 2010.

Dörr, H., Kromer, B., Levin, I., Münnic, K. O., and Volpp, H.-J.: CO_2 and radon 222 as tracers for atmospheric transport, J. Geophys. Res., 88, 1309–1313, doi:10.1029/JC088iC02p01309, 1983.

Druffel, E. M. and Suess, H. E.: On the radiocarbon record in banded corals: exchange parameters and net transport of $^{14}CO_2$ between atmosphere and surface ocean, J. Geophys. Res.-Oceans, 88, 1271–1280, 1983.

European Commission: Joint Research Centre/PBL Netherlands Environmental Assessment Agency. The Emissions Database for Global Atmospheric Research (EDGAR) version 4.3, available at: http://edgar.jrc.ec.europa.eu/, last access: 22 July 2015.

Esler, M. B., Griffith, D. W. T., Wilson, S. R., and Steele, L. P.: Precision trace gas analysis by FT-IR spectroscopy. 2. The $^{13}C / ^{12}C$ isotope ratio of CO_2, Anal. Chem., 72.1, 216-221, 2000.

Flanagan, L. B., Ehleringer, J. R., and Pataki D. E. (Eds.): Stable isotopes and biosphere-atmosphere interactions, Elsevier Academic Press, San Diego, US, 318 pp., 2005.

ACPD
15, 20181–20243, 2015

Gamnitzer, U., Karstens, U., Kromer, B., Neubert, R. E., Meijer, H. A., Schroeder, H., and Levin, I.: Carbon monoxide: A quantitative tracer for fossil fuel CO_2?, J. Geophys. Res.-Atmos., 111, D22302, doi:10.1029/2005JD006966, 2006.

Gerbig, C., Lin, J. C., Wofsy, S. C., Daube, B. C., Andrews, A. E., Stephens, B. B., Bakwin, P. S., and Grainger, C. A.: Toward constraining regional-scale fluxes of CO_2 with atmospheric observations over a continent: 2. Analysis of COBRA data using a receptor-oriented framework, J. Geophys. Res.-Atmos., 108, 4757, doi:10.1029/2003JD003770, 2003.

Gerbig, C., Lin, J. C., Munger, J. W., and Wofsy, S. C.: What can tracer observations in the continental boundary layer tell us about surface-atmosphere fluxes?, Atmos. Chem. Phys., 6, 539–554, doi:10.5194/acp-6-539-2006, 2006.

Graven, H. D. and Gruber, N.: Continental-scale enrichment of atmospheric $^{14}CO_2$ from the nuclear power industry: potential impact on the estimation of fossil fuel-derived CO_2, Atmos. Chem. Phys., 11, 12339–12349, doi:10.5194/acp-11-12339-2011, 2011.

Gros, V., Tsigaridis, K., Bonsang, B., Kanakidou, M., and Pio, C.: Factors controlling the diurnal variation of CO above a forested area in southeast Europe, Atmos. Environ., 36, 3127–3135, 2002.

Gurney, K. R., Law, R. M., Denning, A. S., Rayner, P. J., Baker, D., Bousquet, P., Bruhwiler, L., Chen, Y.-H., Ciais, P., Fan, S., Fung, I. Y., Gloor, M., Heimann, M., Higuchi, K., John, J., Maki, T., Maksyutov, S., Masarie, K., Peylin, P., Prather, M., Pak, B., Randerson, J., Sarmiento, J., Taguchi, S., Takahashi, T., and Yuen, C.-W.: Towards robust regional estimates of CO_2 sources and sinks using atmospheric transport models, Nature, 415, 626–630, 2002.

Gurney, K. R., Chen, Y.-H., Maki, T., Kawa, S. R., Andrews, A., and Zhu, Z.: Sensitivity of atmospheric CO_2 inversions to seasonal and interannual variations in fossil fuel emissions, J. Geophys. Res., 110, D10308, doi:10.1029/2004JD005373, 2005.

Hammer, S., Griffith, D. W. T., Konrad, G., Vardag, S., Caldow, C., and Levin, I.: Assessment of a multi-species in situ FTIR for precise atmospheric greenhouse gas observations, Atmos. Meas. Tech., 6, 1153–1170, doi:10.5194/amt-6-1153-2013, 2013.

Heimann, M. and Koerner, S.: The global atmospheric tracer model TM3, Technical Reports, Max-Planck-Institute for Biogeochemie, 5, 131 pp., 2003.

Inman, R. E., Ingersoll, R. B., and Levy, E. A.: Soil: A natural sink for carbon monoxide, Science, 172, 1229–1231, doi:10.1126/science.172.3989.1229, 1971.

Jung, M., Henkel, K., Herold, M., and Churkina, G.: Exploiting synergies of global land cover products for carbon cycle modeling, Remote Sens. Environ., 101, 534–553, 2006.

ACPD
15, 20181–20243, 2015

Kaul, M.: Isotopenverhältnisse im atmosphärischem Kohlendioxid und seine Quellen im Raum Heidelberg, Staatsexamensarbeit, 2007.

Keeling, C. D.: The concentration and isotopic abundances of atmospheric carbon dioxide in rural areas, Geochim. Cosmochim. Ac., 13, 322–334, 1958.

Keeling, C. D.: The concentration and isotopic abundance of carbon dioxide in rural and marine air, Geochim. Cosmochim. Ac., 24, 277–298, 1961.

Keeling, R. F., Piper, S. C., and Heimann, M.: Global and hemispheric CO_2 sinks deduced from changes in atmospheric O_2 concentration, Nature, 381, 218–221, 1996.

Le Quéré, C., Moriarty, R., Andrew, R. M., Peters, G. P., Ciais, P., Friedlingstein, P., Jones, S. D., Sitch, S., Tans, P., Arneth, A., Boden, T. A., Bopp, L., Bozec, Y., Canadell, J. G., Chini, L. P., Chevallier, F., Cosca, C. E., Harris, I., Hoppema, M., Houghton, R. A., House, J. I., Jain, A. K., Johannessen, T., Kato, E., Keeling, R. F., Kitidis, V., Klein Goldewijk, K., Koven, C., Landa, C. S., Landschützer, P., Lenton, A., Lima, I. D., Marland, G., Mathis, J. T., Metzl, N., Nojiri, Y., Olsen, A., Ono, T., Peng, S., Peters, W., Pfeil, B., Poulter, B., Raupach, M. R., Regnier, P., Rödenbeck, C., Saito, S., Salisbury, J. E., Schuster, U., Schwinger, J., Séférian, R., Segschneider, J., Steinhoff, T., Stocker, B. D., Sutton, A. J., Takahashi, T., Tilbrook, B., van der Werf, G. R., Viovy, N., Wang, Y.-P., Wanninkhof, R., Wiltshire, A., and Zeng, N.: Global carbon budget 2014, Earth Syst. Sci. Data, 7, 47–85, doi:10.5194/essd-7-47-2015, 2015.

Levin, I. and Karstens, U.: Inferring high-resolution fossil fuel CO_2 records at continental sites from combined (CO_2)-C-14 and CO observations, Tellus B, 59, 245–250, doi:10.1111/j.1600-0889.2006.00244.x, 2007.

Levin, I., Kromer, B., Schmidt, M., and Sartorius, H.: A novel approach for independent budgeting of fossil fuel CO_2 over Europe by $^{14}CO_2$ observations, Geophys. Res. Lett., 30, 2194, doi:10.1029/2003GL018477, 2003.

Levin, I., Hammer, S., Kromer, B., Meinhardt, F.: Radiocarbon observations in atmospheric CO_2: Determining fossil fuel CO_2 over Europe using Jungfraujoch observations as background, Sci. Total Environ., 391, 211–216, 2008.

Levin, I., Naegler, T., Kromer, B., Diehl, M., Francey, R. J., Gomez-Pelaez, A. J., Steele, L. P., Wagenbach, D., Weller, R., and Worthy, D. E.: Observations and modelling of the global distribution and long-term trend of atmospheric $^{14}CO_2$, Tellus B, 62, 26–46, 2010.

Levin, I., Kromer, B., and Hammer, S.: Atmoposheric $\Delta^{14}CO_2$ trend in Western European background air from 2000 to 2012, Tellus B, 65, 20092, doi:10.3402/tellusb.v65i0.20092, 2013.

ACPD
15, 20181–20243, 2015

Lin, J. C., Gerbig, C., Wofsy, S. C., Andrews, A. E., Daube, B. C., Davis, K. J., and Grainger, C. A.: A near-field tool for simulating the upstream influence of atmospheric observations: The Stochastic Time-Inverted Lagrangian Transport (STILT) model, J. Geophys. Res., 108, 4493, doi:10.1029/2002JD003161, 2003.

Mahadevan, P., Wofsy, S. C., Matross, D. M., Xiao, X., Dunn, A. L., Lin, J. C., Gerbig, C., Munger, J. W., Chow, V. Y., and Gottlieb, E. W.: A satellite-based biosphere parameterization for net ecosystem CO_2 exchange: Vegetation Photosynthesis and Respiration Model (VPRM), Global Biogeochem. Cy., 22, GB2005, doi:10.1029/2006GB002735, 2008.

Marland, G., Brenkert, A., and Olivier, J.: CO_2 from fossil fuel burning: a comparison of ORNL and EDGAR estimates of national emissions, Environ. Sci. Pol., 2, 265–273, doi:10.1016/s1462-9011(99)00018-0, 1999.

McIntyre, C. P., McNicholm, A. P., Roberts, M. L., Seewald, J. S., von Reden, K. F., and Jenkins, W. J.: Improved Precision of ^{14}C Measurements for CH_4 and CO_2 Using GC and Continuous-Flow AMS Achieved by Summation of Repeated Injections, Radiocarbon, 55, 677–685, 2013.

Meijer, H. A. J., Smid, H. M., Perez, E., Keizer, M. G.: Isotopic characterization of anthropogenic CO_2 emissions using isotopic and radiocarbon analysis, Phys. Chem. Earth, 21, 483–487, 1996.

Miller, J. B., Lehman, S. J., Montzka, S. A., Sweeney, C., Miller, B. R., Karion, A., Wolak, C., Dlugokencky, E. J., Southon, J., Turnbull, J. C., and Tans, P. P.: Linking emissions of fossil fuel CO_2 and other anthropogenic trace gases using atmospheric $^{14}CO_2$, J. Geophys. Res., 117, D08302, doi:10.1029/2011JD017048, 2012.

Mook, W. M. E.: Environmental Isotopes in the Hydrological Cycle. Principles and Applications, UNESCO/IAEA Series, available at: http://www.hydrology.nl/ihppublications/149-environmental-isotopes-in-the-hydrological-cycle-principles-and-applications.html (last access: 22 July 2015), 2001.

Newman, S., Jeong, S., Fischer, M. L., Xu, X., Haman, C. L., Lefer, B., Alvarez, S., Rappenglueck, B., Kort, E. A., Andrews, A. E., Peischl, J., Gurney, K. R., Miller, C. E., and Yung, Y. L.: Diurnal tracking of anthropogenic CO_2 emissions in the Los Angeles basin megacity during spring 2010, Atmos. Chem. Phys., 13, 4359–4372, doi:10.5194/acp-13-4359-2013, 2013.

Nydal, R., Lövseth, K., and Gullicksen, S.: A survey of radiocarbon variation in nature since the test ban treaty, University of California Press, Berkley, California, 1979.

ACPD
15, 20181–20243, 2015

Parrish, D. D., Trainer, M., Holloway, J. S., Yee, J., Warshawsky, S., Fehsenfeld, F., Forbes, G., and Moody, J.: Relationships between ozone and carbon monoxide at surface sites in the North Atlantic region, J. Geophys. Res., 103, 13357–13376, doi:10.1029/98JD00376, 1993.

Pataki, D. E., Ehleringer, J. R., Flanagan, L. B., Yakir, D., Bowling, D. R., Still, C. J., Buchmann, N. , Kaplan, J. O., and Berry, J. A.: The application and interpretation of Keeling plots in terrestrial carbon cycle research, Global Biogeochem. Cy., 17, 1022, doi:10.1029/2001GB001850, 2003.

Pataki, D. E., Alig, R. J., Fung, A. S., Golubiewski, N. E., Kennedy, C. A., McPherson, E. G., Nowak, D. J., Pouyat, R. V., and Romero Lankao, P.: Urban ecosystems and the North American carbon cycle, Glob. Change Biol., 12, 2092–2102, doi:10.1111/j.1365-2486.2006.01242.x, 2006.

Peylin, P., Houweling, S., Krol, M. C., Karstens, U., Rödenbeck, C., Geels, C., Vermeulen, A., Badawy, B., Aulagnier, C., Pregger, T., Delage, F., Pieterse, G., Ciais, P., and Heimann, M.: Importance of fossil fuel emission uncertainties over Europe for CO_2 modeling: model intercomparison, Atmos. Chem. Phys., 11, 6607–6622, doi:10.5194/acp-11-6607-2011, 2011.

Peylin, P., Law, R. M., Gurney, K. R., Chevallier, F., Jacobson, A. R., Maki, T., Niwa, Y., Patra, P. K., Peters, W., Rayner, P. J., Rödenbeck, C., van der Laan-Luijkx, I. T., and Zhang, X.: Global atmospheric carbon budget: results from an ensemble of atmospheric CO_2 inversions, Biogeosciences, 10, 6699–6720, doi:10.5194/bg-10-6699-2013, 2013.

Prather, M., Ehhalt, D., Dentener, F., Derwent, R. G., Dlugokencky, E., Holland, E., Isaksen, I. S. A., Katima, J., Kirchhoff, V., Matson, P., Midgley, P. M., and Wang, M.: Atmospheric chemistry and greenhouse gases, in: Climate Change 2001, edited by: Houghton, J. T., 239–287, Cambridge Univ. Press, New York, 2001.

Rödenbeck, C.: Estimating CO_2 sources and sinksfrom atmospheric mixing ratio measurements using a global inversion of atmospheric transport, Max Planck Institute for Biogeochemistry, Jena, Germany, available at: http://www.bgc-jena.mpg.de/bgc-systems/pmwiki2/uploads/Publications/6.pdf (last access: 22 July 2015), 2005.

Rogelj, J., McCollum, D., Smith, S., Calvin, K., Clarke, L., Garg, A., Jiang, K., Krey, V., Lowe, J., Riahi, K., Schaeffer, M., van Vuuren, D., Wenying, C., Crippa, M., and Janssens-Maenhout, G.: Chapter 2 of The emission gap report 2014: What emission levels will comply with temperature limit, in: The emission gap report 2014: a UNEP synthesis report, United Nations Environment Programme (UNEP), November 2014, Nairobi, 2014.

ACPD
15, 20181–20243, 2015

Rivier, L., Ciais, P., Hauglustaine, D. A., Bakwin, P., Bousquet, P., Peylin, P., and Klonecki, A.: Evaluation of SF_6, C_2Cl_4 and CO to approximate fossil fuel CO_2 in the Northern Hemisphere using a chemistry transport model, J. Geophys. Res., 111, D16311, doi:10.1029/2005JD006725, 2006.

Schmidt, A., Rella, C. W., Göckede, M., Hanson, C., Yang, Z., and Law, B. E.: Removing traffic emissions from CO_2 time series measured at a tall tower using mobile measurements and transport modeling, Atmos. Environ., 97, 94–108, doi:10.1016/j.atmosenv.2014.08.006, 2014.

Steinbach, J., Gerbig, C., Rödenbeck, C., Karstens, U., Minejima, C., and Mukai, H.: The CO_2 release and Oxygen uptake from Fossil Fuel Emission Estimate (COFFEE) dataset: effects from varying oxidative ratios, Atmos. Chem. Phys., 11, 6855–6870, doi:10.5194/acp-11-6855-2011, 2011.

Stohl, A., Forster, C., Frank, A., Seibert, P., and Wotawa, G.: Technical note: The Lagrangian particle dispersion model FLEXPART version 6.2, Atmos. Chem. Phys., 5, 2461–2474, doi:10.5194/acp-5-2461-2005, 2005.

Stuiver, M. and Polach, H. A.: Reporting of C-14 data-Discussion, Radiocarbon, 19, 355–363, 1977.

Stuiver, M. and Quay, P. D.: Atmospheric ^{14}C changes resulting from fossil fuel CO_2 release and cosmic ray flux variability, Earth Planet. Sc. Lett., 53, 349–362, 1981.

Suess, H. E: Radiocarbon concentration in modern wood, Science, 122, 415–417, 1955.

Taylor, A. J., Lai, C. T., Hopkins, F. M., Wharton, S., Bible, K., Xu, X., Philipps, C., Bush, S., and Ehleringer, J. R.: Radiocarbon-Based Partitioning of Soil Respiration in an Old-Growth Coniferous Forest, Ecosystems, 18, 1–12, 2015.

Trusilova, K., Rödenbeck, C., Gerbig, C., and Heimann, M.: Technical Note: A new coupled system for global-to-regional downscaling of CO_2 concentration estimation, Atmos. Chem. Phys., 10, 3205–3213, doi:10.5194/acp-10-3205-2010, 2010.

Turnbull, J. C., Miller, J. B., Lehman, S. J., Tans, P. P., Sparks, R. J., and Southon, J.: Comparison of $^{14}CO_2$, CO, and SF_6 as tracers for recently added fossil fuel CO_2 in the atmosphere and implications for biological CO_2 exchange, Geophys. Res. Lett., 33, L01817, doi:10.1029/2005GL024213, 2006.

Turnbull, J. C., Sweeney, C., Karion, A., Newberger, T., Lehman, S. J., Tans, P. P., Davis, K. J., Lauvaux, T., Miles, N. L., Richardson, S. J., Cambaliza, M. O., Shepson, P. B., Gurney, K., Patarasuk, R., and Razlivanov, I.: Toward quantification and source sector identification

ACPD
15, 20181–20243, 2015

of fossil fuel CO_2 emissions from an urban area: Results from the INFLUX experiment, J. Geophys. Res.-Atmos., 120, 292–312, doi:10.1002/2014JD022555, 2015.

Tuzson, B., Henne, S., Brunner, D., Steinbacher, M., Mohn, J., Buchmann, B., and Emmenegger, L.: Continuous isotopic composition measurements of tropospheric CO_2 at Jungfraujoch (3580 m a.s.l.), Switzerland: real-time observation of regional pollution events, Atmos. Chem. Phys., 11, 1685–1696, doi:10.5194/acp-11-1685-2011, 2011.

Vardag, S. N., Hammer, S., O'Doherty, S., Spain, T. G., Wastine, B., Jordan, A., and Levin, I.: Comparisons of continuous atmospheric CH_4, CO_2 and N_2O measurements – results from a travelling instrument campaign at Mace Head, Atmos. Chem. Phys., 14, 8403–8418, doi:10.5194/acp-14-8403-2014, 2014.

Vogel, F. R.: $^{14}CO_2$-calibrated carbon monoxide as proxy to estimate the regional fossil fuel CO_2 component at hourly resolution, PhD thesis, Ruprecht-Karls University Heidelberg, Germany, 2010.

Vogel, F. R., Hammer, S., Steinhof, A., Kromer, B., and Levin, I.: Implication of weekly and diurnal ^{14}C calibration on hourly estimates of CO-based fossil fuel CO_2 at a moderately polluted site in southwestern Germany, Tellus B, 62, 512–520, doi:10.3402/tellusb.v62i5.16600, 2010.

Vogel, F. R., Huang, L., Ernst, D., Giroux, L., Racki, S., and Worthy, D. E. J.: Evaluation of a cavity ring-down spectrometer for in situ observations of $^{13}CO_2$, Atmos. Meas. Tech., 6, 301–308, doi:10.5194/amt-6-301-2013, 2013a.

Vogel, F. R., Levin, I., and Worthy, D.: Implications for Deriving Regional Fossil Fuel CO_2 Estimates from Atmospheric Observations in a Hot Spot of Nuclear Power Plant $^{14}CO_2$ Emissions, Radiocarbon, 55, 1556–1572, doi:10.2458/azu_js_rc.55.16347, 2013b.

Wang, R., Tao, S., Ciais, P., Shen, H. Z., Huang, Y., Chen, H., Shen, G. F., Wang, B., Li, W., Zhang, Y. Y., Lu, Y., Zhu, D., Chen, Y. C., Liu, X. P., Wang, W. T., Wang, X. L., Liu, W. X., Li, B. G., and Piao, S. L.: High-resolution mapping of combustion processes and implications for CO_2 emissions, Atmos. Chem. Phys., 13, 5189–5203, doi:10.5194/acp-13-5189-2013, 2013.

Widory, D., Proust, E., Bellenfant, G., and Bour, O.: Assessing methane oxidation under landfill covers and its contribution to the above atmospheric CO_2 levels: The added value of the isotope ($\delta^{13}C$ and $\delta^{18}O$ CO_2; $\delta^{13}C$ and δD CH_4) approach, Waste Manage, 32, 1685–1692, 2012.

ACPD
15, 20181–20243, 2015

Zondervan, A. and Meijer, H. A. J.: Isotopic characterisation of CO_2 sources during regional pollution events using isotopic and radiocarbon analysis, Tellus B, 48, 601–612, doi:10.1034/j.1600-0889.1996.00013.x, 1996.

ACPD
15, 20181–20243, 2015

Table 1. $\delta^{13}C(CO_2)$ source signature of fuel types and biosphere as used in the model. The isotopic signature of the biosphere follows the findings of Ballantyne et al. (2011) for Europe. The assigned isotopic fuel values were chosen from mean measured isotopic signatures in Heidelberg (Kaul, 2007 and unpublished data) or if not available, are similar to isotopic $\delta^{13}C(CO_2)$ values reported in Andres et al. (1994) or (for biogas) Widory et al. (2012).

Emission source	$\delta_{ff,i}$, $\delta_{bf,j}$ or δ_{bio} [‰]
Hard coal	−27
Brown coal	−29
Peat	−30
Solid waste	−30
Heavy oil	−31
Light oil	−31
Natural gas	−48
Derived gas	−30
Solid biomass	−29
Bio liquid	−31
Biosphere	
Jan	−27
Feb	−26
Mar	−25
Apr	−24
May	−23
Jun	−22
Jul	−22
Aug	−23
Sep	−24
Oct	−25
Nov	−26
Dec	−27

ACPD
15, 20181–20243, 2015

Table 2. Tracer or tracer combinations, required parameters and formula for estimation of targeted fuel CO_2 concentration. In cases (c) and (d) we further divide fuel CO_2 into traffic CO_2 and non-traffic CO_2, or fossil fuel CO_2 and biofuel CO_2, respectively. In case (f) we can only estimate fossil fuel CO_2 with $\Delta^{14}C(CO_2)$ and therefore lack biofuel CO_2 for a comprehensive fuel CO_2 estimate.

Case	Required parameters	Formula (for derivation see Appendix A1)
(a) CO_2		$y_F = \Delta y$
(b) CO	$\overline{R_F}$	$y_F = \frac{\Delta x}{\overline{R_F}}$
(c) CO(tr) + $\delta^{13}C(CO_2)$	$\overline{R_{tr}}$, $\overline{m_{tr}}$, $\overline{\delta_{tr}}$, $\overline{\delta_{F\text{-}tr}}$	$y_F = \frac{\Delta x(t)\cdot\overline{m_{tr}}}{\overline{R_{tr}}} + \frac{y_{tot}\delta_{tot} - y_{bg}\delta_{bg} - (y_{tot} - y_{bg} - y_{tr})\delta_{bio} - y_{tr}\overline{\delta_{tr}}}{\overline{\delta_{F\text{-}tr}} - \delta_{bio}}$
(d) CO(bf) + $\delta^{13}C(CO_2)$	$\overline{R_{bf}}$, $\overline{m_{bf}}$, $\overline{\delta_{bf}}$, $\overline{\delta_{ff}}$	$y_F = \frac{\Delta x(t)\cdot\overline{m_{bf}}}{\overline{R_{bf}}} + \frac{y_{tot}\delta_{tot} - y_{bg}\delta_{bg} - (y_{tot} - y_{bg} - y_{bf})\delta_{bio} - y_{bf}\overline{\delta_{bf}}}{\overline{\delta_{ff}} - \delta_{bio}}$
(e) $\delta^{13}C(CO_2)$	$\overline{\delta_F}$	$y_F = \frac{y_{tot}\delta_{tot} - y_{bg}\delta_{bg} - (y_{tot} - y_{bg})\delta_{bio}}{\overline{\delta_F} - \delta_{bio}}$
(f) $\Delta^{14}C(CO_2)$	$\Delta^{14}C_{bf}$, $\Delta^{14}C_{bio}$	$y_F \approx y_{ff} = \frac{y_{bg}(\Delta^{14}C_{bg} - \Delta^{14}C_{bio}) - y_{tot}(\Delta^{14}C_{tot} - \Delta^{14}C_{bio}) - y_{bf}(\Delta^{14}C_{bio} - \Delta^{14}C_{bf})}{1 + \Delta^{14}C_{bio}}$

ACPD
15, 20181–20243, 2015

Table 3. Mean difference of tracer-based estimate and modelled (as correct assumed) fuel CO_2 in µmol mol^{-1} for the tracers CO and $\delta^{13}C(CO_2)$ for different sampling strategies and respective standard deviation (both determined from a Gaussian fit to the difference histogram) for an urban setting (here: Heidelberg). Depending on the random selection of grab samples, the bias of the calibration with annualy distributed grab samples is sometimes positive and sometimes negative. Therefore, the mean absolute difference between the modelled and calibrated value was determined in a Monte-Carlo simulation and is denoted with a "±" in front of the mean value to show that the bias does not have a unique sign. The standard deviation denotes the 1σ uncertainty of the difference, which is always bi-directional. Note, that we only show the results for CO and $\delta^{13}C(CO_2)$, since the results when using a combination of these tracers is very similar to those of the $\delta^{13}C(CO_2)$-method. Measurement uncertainties are included in all calibration methods.

Method		CO-Method		$\delta^{13}C(CO_2)$-Method	
		Summer	Winter	Summer	Winter
No uncertainties, monthly median values known (as shown in Fig. 1)		−0.1 ± 0.7	−0.2 ± 1.1	0.0 ± 0.7	0.1 ± 1.0
Measurement uncertainties included, monthly median values known (as shown in Fig. 5)		−0.2 ± 4.9	−0.3 ± 4.8	−0.1 ± 3.4	−0.4 ± 4.3
Calibration with integrated samples (method 1)	$n = 24$	−1.5 ± 6.5	−1.2 ± 5.2	−3.0 ± 7.0	−2.3 ± 5.0
Calibration with annually distributed grab samples (method 2)	$n = 24$ $n = 96$	±0.9 ± 5.7 ±0.6 ± 5.4	±1.4 ± 5.2 ±1.1 ± 5.0	±0.7 ± 4.4 ±0.4 ± 4.1	±1.3 ± 4.8 ±0.9 ± 4.6
Calibration with seasonal grab sample calibration (method 3)	$n = 24$ $n = 96$	±1.1 ± 5.9 ±0.6 ± 5.4	±1.5 ± 5.3 ±1.0 ± 4.9	±1.0 ± 4.7 ±0.3 ± 4.1	±1.5 ± 5.3 ±0.9 ± 4.6
Seasonal event calibration (method 4)	$n = 24$ $n = 96$	±1.1 ± 6.0 ±1.2 ± 6.2	±1.5 ± 5.3 ±1.8 ± 5.4	±0.9 ± 4.5 ±0.4 ± 4.2	±1.5 ± 5.0 ±1.0 ± 4.6

ACPD
15, 20181–20243, 2015

Table A1. Annual or half-yearly (summer = S, winter = W) averaged $\Delta^{14}C(CO_2)$, $\delta^{13}C(CO_2)$, $\Delta CO / \Delta CO_2$ ratios and mean fraction of CO_2 and CO relative to total CO_2 and CO offsets as used in our model study for the measurement site Heidelberg for the year 2012. Biosphere $\Delta^{14}C(CO_2)$ values are based on Taylor et al. (2015). The $\Delta CO / \Delta CO_2$ ratio and the fractions of CO_2 and CO offset were taken from the STILT model runs, which were fed with anthropogenic emissions from the EDGAR emission inventory. Note, that fractions of biofuels in traffic CO_2 emissions are not included. δ values were derived by assigning an isotopic value to each fuel type and weighting these depending on the respective share of the fuel type to total fuel CO_2 at the measurement site. The δ values of the biosphere are the half-yearly mean values from Table 1. Analogously, R_x (and $\Delta^{14}C_x$) values were derived by assigning an emission ratio CO / CO_2 (and $\Delta^{14}C(CO_2)$ value) to each emission sector and weighting these depending on the respective share of the emission sector to total fuel CO_2 at the site. The two main sector fuel CO_2 and bioshperic CO_2 are written in bolt and add up to 100 %.

Emission group	$\Delta^{14}C(CO_2)$ [‰]	$\delta^{13}C$ [‰]		$\overline{R}_x = (\Delta CO / \Delta CO_2)_x$ $[(\text{nmol mol})^{-1}$ $(\mu\text{mol mol}^{-1})^{-1}]$	% of ΔCO_2		% of ΔCO	
		S	W		S	W	S	W
Fuel CO_2	−995	−31.5	−33.5	4	**50**	**80**	**100**	**100**
Fossil fuel CO_2 (excl. biofuels)	−1000	−32	−34	2	45	70	50	37
Biofuel CO_2	90	−27	−28	19	5	10	$\overline{m}_{bf} = 50$	$\overline{m}_{bf} = 63$
Fuel CO_2 excl. traffic CO_2 (but incl. biofuels)	−990	−31.5	−33.8	4	35	67	70	80
Traffic fuel CO_2	−1000	−31	−31	4	15	13	$\overline{m}_{tr} = 30$	$\overline{m}_{tr} = 20$
Biospheric CO_2	60	−23	−25.5	0	**50**	**20**	**0**	**0**

ACPD
15, 20181–20243, 2015

Table A2. List of acronyms

AMS	accelerator mass spectrometry
bf	Biofuel
bg	Background
bio	Biosphere
EDGAR	Emissions Database for Global Atmospheric Research
F	Fuel
F-bf	Fuel excluding biofuels (= ff)
ff	Fossil fuel
F-tr	Fuel excluding traffic
GC	Gas chromatography
ICOS	Integrated Carbon Observation System
IQR	Inter-quartile range
m_x	CO share of emission group x to CO offset
NPP	Nuclear power plant
ppm	parts per million, equivalent to μmol mol^{-1}
ppb	parts per billion, equivalent to nmol mol^{-1}
R_x	Ratio of CO to CO_2 in the emission group x
SD	Standard deviation
STILT	Stochastic Time-Inverted Langrangian Particle model
tot	Total
x	CO mole fraction
y	CO_2 mole fraction

ACPD
15, 20181–20243, 2015

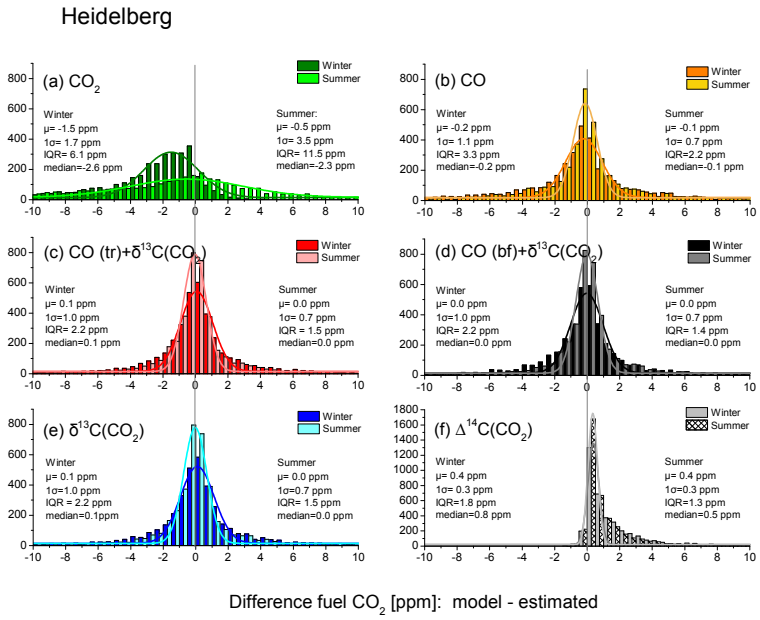

Figure 1. Histograms showing the differences between the modeled fuel CO_2 (assumed as correct) and the tracer-based estimated fuel CO_2 for the year 2012 for Heidelberg using the different tracers and tracer configurations listed in Table 2. Differences result from sub-monthly variations of parameters. Note the different *y* axis scale. Darker colors denote the winter periods and lighter colors the summer periods (see legend). The distributions were fitted with a Gaussian fit and the shift (μ) and the standard deviation (σ) for the Gaussian fits are given in the figure. Since the histograms do not follow Gaussian distributions (especially for $^{14}C(CO_2)$ due to not normally distributed biofuel CO_2 contributions within one year) we also give the Interquartile range (IQR) in the figure to remind the reader that the uncertainty may be underestimated when using the Gaussian standard deviation for uncertainty analysis. The CO_2 mole fractions are given in parts per million (ppm), which is equivalent to μmol mol^{-1}. Note that in Heidelberg, mean fuel CO_2 for summer is 15 μmol mol^{-1} and for winter is 16 μmol mol^{-1}.

ACPD
15, 20181–20243, 2015

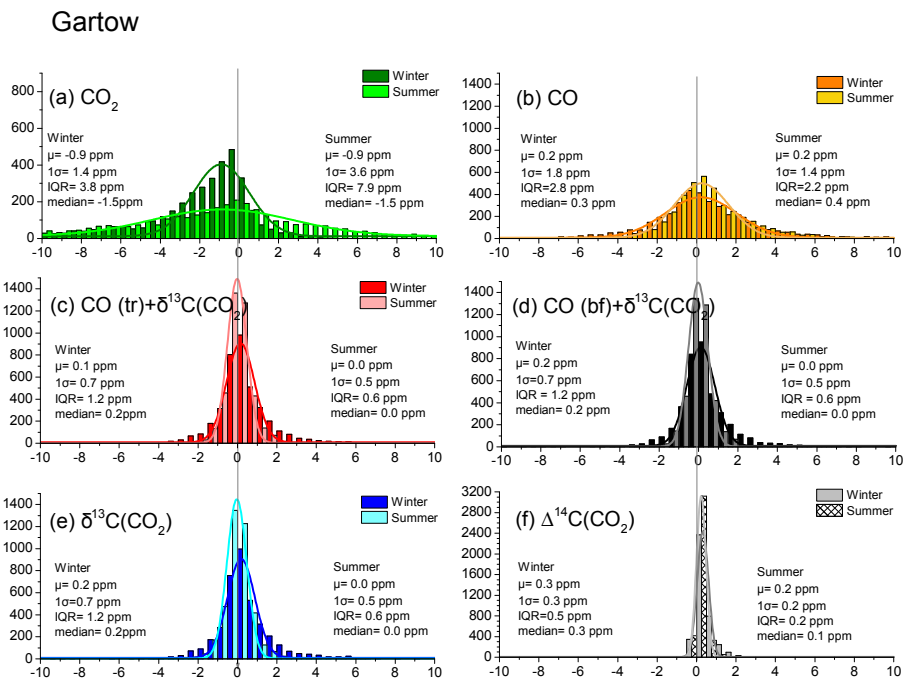

Figure 2. Same as Fig. 1, but for Gartow. In Gartow, mean fuel CO_2 for summer is 2 µmol mol^{-1} and for winter is 4 µmol mol^{-1}.

ACPD
15, 20181–20243, 2015

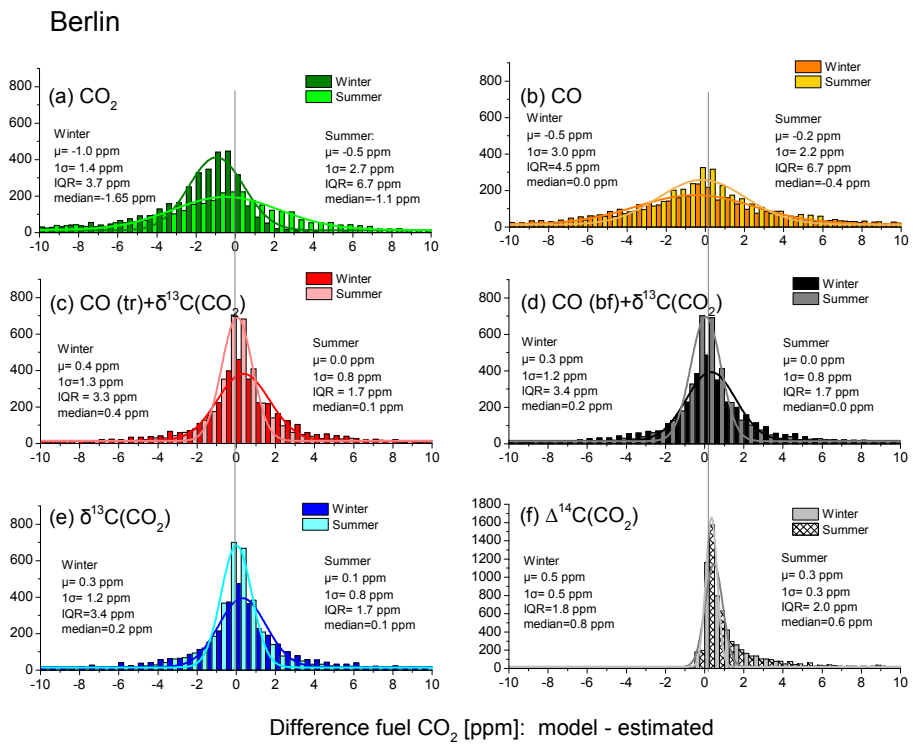

Figure 3. Same as Fig. 1, but for Berlin. In Berlin, mean fuel CO_2 for summer is 23 µmol mol^{-1} and for winter is 27 µmol mol^{-1}.

ACPD
15, 20181–20243, 2015

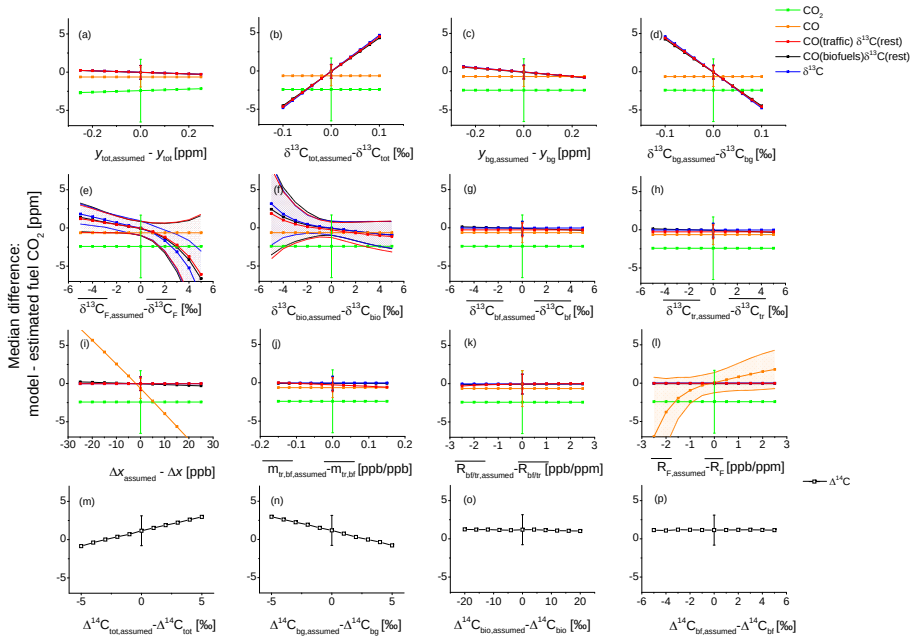

Figure 4. Sensitivity analysis: Median difference between the modelled fuel CO_2 and the tracer-based estimated fuel CO_2 value (y axis) at a typical urban site (Heidelberg) when using parameters/variables for fuel CO_2 estimation ("assumed") deviating from the correct parameters/variables used in STILT. The error bars given at $x = 0$ (assumed value = model value) denote the Inter-quartile ranges (IQR) for all x positions. If the IQRs vary depending on the assumed value, the errors (IQRs) are drawn as shaded areas.

ACPD
15, 20181–20243, 2015

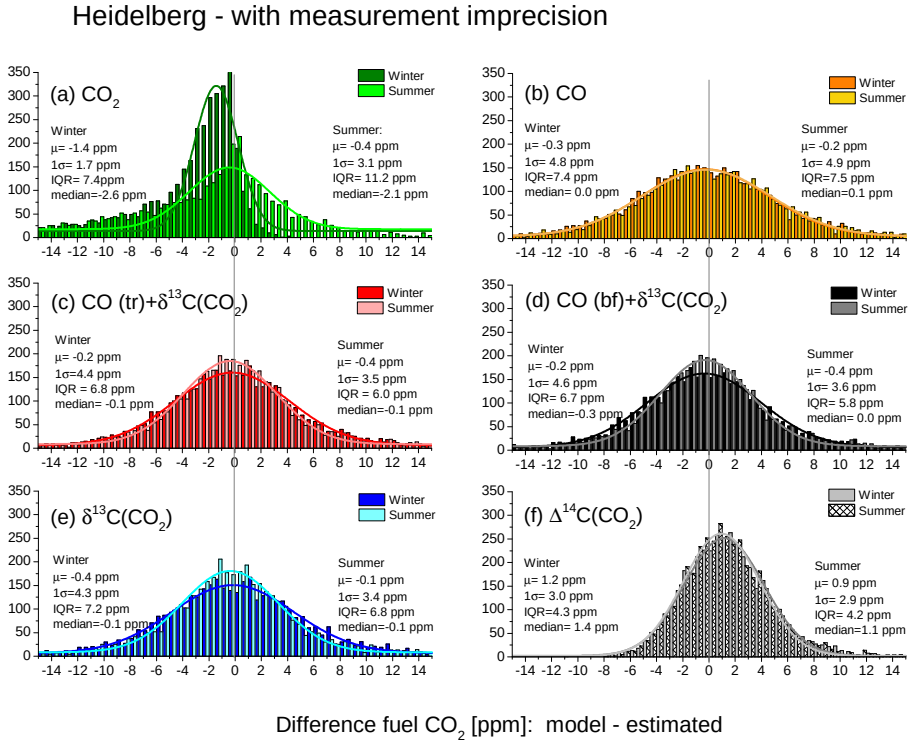

Figure 5. Same as Fig. 1, but now also including measurement imprecision.

ACPD
15, 20181–20243, 2015

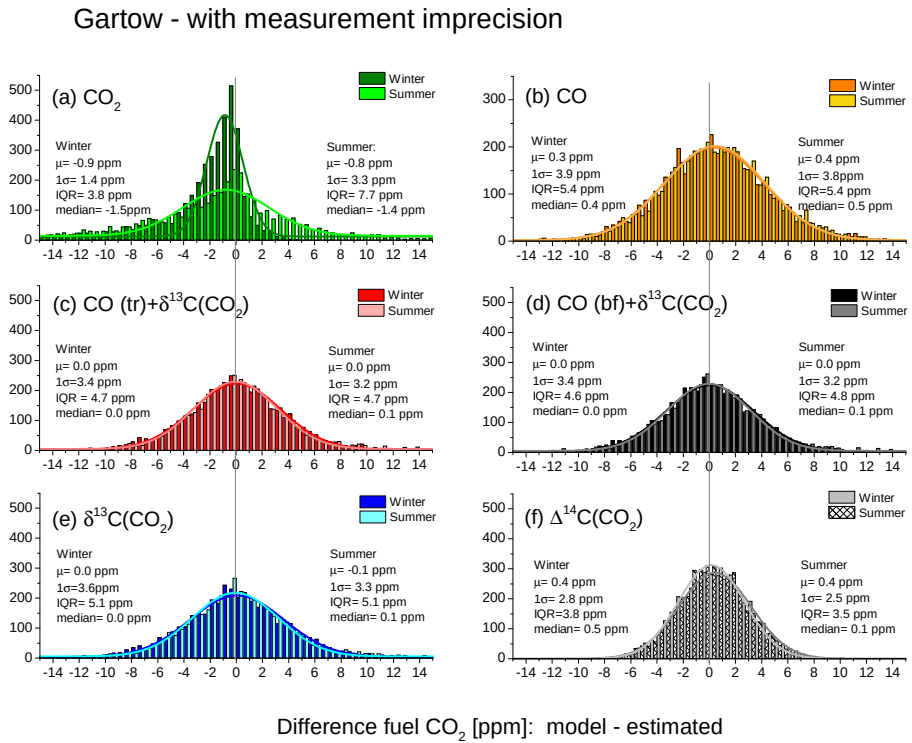

Figure 6. Same as Fig. 2, but now also including measurement imprecision.

ACPD
15, 20181–20243, 2015

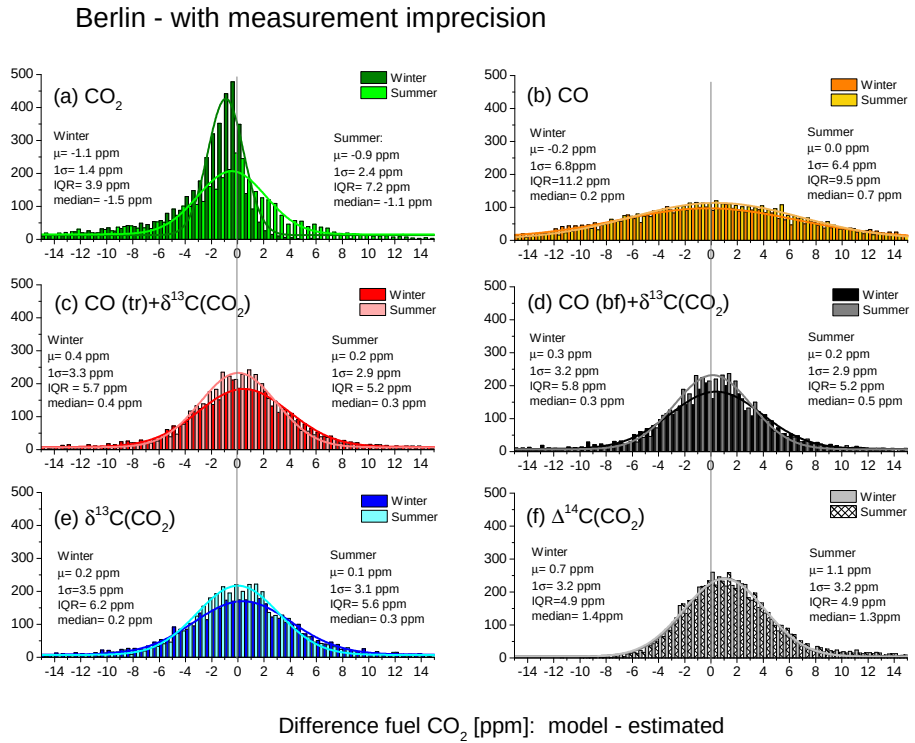

Figure 7. Same as Fig. 3, but now also including measurement imprecision.

ACPD
15, 20181–20243, 2015

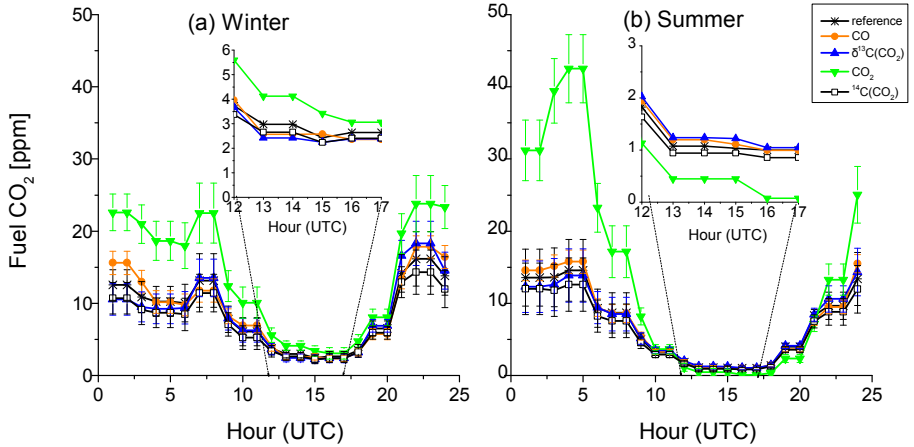

Figure 8. Comparison of median diurnal cycle of fuel CO_2 given in model reference or estimated with one of six different tracer methods at the measurement station Heidelberg. Error bars denote the standard error of the fuel CO_2 estimate at each hour for the respective half year. The diurnal cycle of the CO + $\delta^{13}C(CO_2)$ methods are not shown, since they are very similar to the $\delta^{13}C(CO_2)$ method.

ACPD
15, 20181–20243, 2015

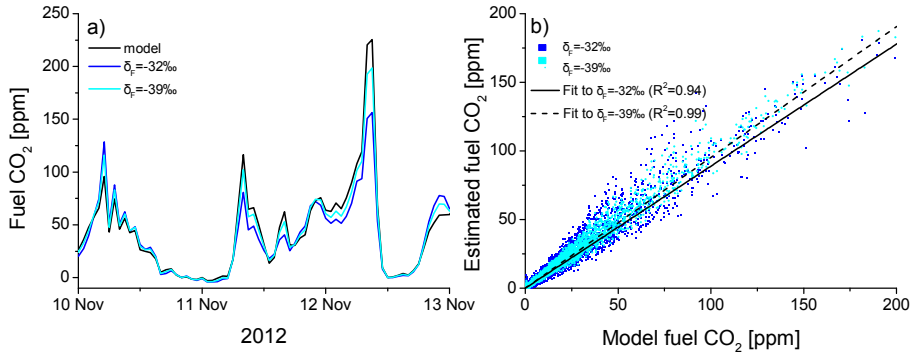

Figure A1. (a) Example period showing fuel CO_2 of different fuel CO_2 estimation methods and reference modelled fuel CO_2. Dark blue: Mean δ_F is −32 ‰, cyan: mean δ_F is −39 ‰. **(b)** Correlation plot between estimated and modelled fuel CO_2 for mean δ_F = −32 ‰ (dark blue and solid line) and mean δ_F = −39 ‰ (cyan and dotted line) during entire year 2012. Fuel CO_2 can be estimated much better using $\delta^{13}C(CO_2)$ when the fuel $\delta^{13}C$ signature is strongly depleted with respect to the biosphere. Note, that the slope slightly changes when using more depleted sources. This is because few high fuel CO_2 peaks span the linear regression and therefore determine the slope to a large degree, but as a general tendency for the Heidelberg data set the high fuel CO_2 peaks exhibit an isotopic signature, which is more enriched as the isotopic signature of the mean fuel source mix.

ACPD
15, 20181–20243, 2015